Bulletin of the Geological Society of Malaysia, Volume 74, November 2022, pp. 85 - 110
DOI: https://doi.org/10.7186/bgsm74202206

Facies and biofacies of the Late Quaternary deposits at west Johor, Malaysia: Indicators for sea-level changes, palaeoshoreline, and palaeonvironment

Abdul Hadi Hashim[1,*], Habibah Jamil[1], Ramlan Omar[2]

[1] Geology Programme, Faculty of Science and Technology, Universiti Kebangsaan Malaysia, 43600 Bangi, Selangor, Malaysia
[2] School of Environmental and Natural Resource Sciences, Faculty of Science and Technology, Universiti Kebangsaan Malaysia, 43600 Bangi, Selangor, Malaysia
* Corresponding author email address: a.hadi.hashim@gmail.com

Abstract: In this study, sedimentological and foraminiferal analyses were conducted on two borehole samples (BH1 = 42 m and BH2 = 39 m) at Pontian in west Johor, Peninsular Malaysia. The sedimentological description established ten facies (A to J). They comprised three associations and two sedimentary environments (i.e., estuary and delta plain). The foraminiferal analysis identified four distinct biofacies through similarity plots of taxonomic compositions and their respective groups for each borehole. Each group was designated as Biofacies Ia to Id for BH1 and IIa to IId for BH2. The deposition began with the formation of a small tidal-dominated estuarine basin in the flooded palaeovalley and the subsequent development of a peat-forming estuarine channel that resulted from the flooding of a supratidal zone. Relative sea-level changes were assumed localised to a basin scale. The maximum limit of tidal influence was benchmarked using a mangrove classification for a terrestrial boundary. Based on the foraminiferal analysis, this study identified a few episodes of flooding events, implying the occurrence of several migrations of the paleoshoreline throughout the sequence that traced the configuration of the maximum paleoshoreline.

Keywords: Biofacies, foraminifera, paleoshoreline, Pontian, Quaternary, sea-level changes

Abstrak: Dalam kajian ini, analisis sedimentologi dan foraminifera telah dijalankan ke atas dua teras gerudi (BH1 = 42 m dan BH2 = 39 meter) yang diperolehi dari Pontian di barat Johor, Semenanjung Malaysia. Dalam pemerihalan sedimentologi, sepuluh fasies enapan (A sehingga J) telah dikenalpasti dan dikelaskan kepada tiga sekutuan fasies yang mewakili sekitaran enapan berbeza (estuari dan dataran delta). Dalam analisis foraminifera, empat biofasies telah dikenalpasti melalui plot kesamaan komposisi taksonomi dan juga melalui kumpulan masing-masing untuk setiap teras gerudi tersebut. Setiap kumpulan telah dinamakan sebagai Biofasies Ia sehingga Id untuk BH1 dan IIa sehingga IId untuk BH2. Proses pengenapan ini ditafsirkan bermula dengan pembentukan lembangan estuari kecil yang didominasi pasang-surut. Ia terletak dalam lembah kuno banjir lalu membentuk alur estuari yang menghasilkan enapan gambut akibat kebanjiran zon supra pasang-surut. Perubahan aras laut relatif telah dianggarkan berlaku pada skala lembangan setempat. Had maksimum pengaruh pasang-surut telah ditentukan dengan menggunakan pengkelasan paya bakau untuk menentukan sempadan daratan. Berdasarkan analisis foraminifera, kajian ini telah dapat mengenalpasti beberapa episod kejadian banjir. Ini menandakan berlakunya beberapa migrasi garis laut kuno di sepanjang jujukan ini seterusnya menunjukkan konfigurasi garis laut kuno yang maksimum.

Kata kunci: Biofasies, foraminifera, pesisir laut kuno, Pontian, Kuaterner, perubahan aras laut

INTRODUCTION

Interpretations of sea-level changes in the Late Quaternary in Peninsular Malaysia are often hampered by inadequate information about two key facets: (1) the history of changes in the relative sea level since the Last Glacial Maximum (LGM), and (2) environmental conditions derived from the corresponding shoreline positions (Ali, 2010). Studies on sea-level changes that affected coastal deposits related to the paloenvironment along the west coast of Peninsular Malaysia during the Quaternary period began only in the last ten years or so (e.g., Horton *et al.*, 2005). It was generally agreed that the sea level was much lower years ago than the current one (Hanebuth *et al.*, 2000; Voris, 2000; Bird *et al.*, 2007).

However, the relationship between Quaternary sea-level fluctuations and coastal environments in Peninsular Malaysia is poorly documented. Sea-level studies (e.g. Sathiamurthy & Voris, 2006; Tam *et al.*, 2018) indicated that a series of Sunda shelf flooding events occurred throughout the Quaternary while paleoennvironmental relevance of relative sea level (RSL) was preliminarily discussed (Parham *et al.*, 2014). Later, Parham (2016) suggested a lower RSL in

0126-6187; 2637-109X / Published by the Geological Society of Malaysia.

Peninsular Malaysia. However, several authors presented evidence of extensive flooding during the Quaternary (Geyh *et al.*, 1979; Tjia, 1992, 1996; Abdullah *et al.*, 2003; Kamaludin, 2003) while Khoo (1996) constructed the only available Quaternary paleogeographic model. Consequently, it remains unclear how the paleoenvironment in this region was affected by changes in sea level. Meanwhile, Heaney (1991) proposed the occurrence of an extensive savannah corridor in the Sundaland during the Last Glacial Period (LGP), and other authors (Bird *et al.*, 2005; Crucifix *et al.*, 2005) suggested an improved interpretation of the existence of open vegetation after savannah.

Geological models were synthesised using existing paleobiological datasets for the Quaternary. They included the paleoenvironmental reconstruction of Pliocene Research, Interpretation and Synoptic Mapping (PRISM) models (Dowsett *et al.*, 2016), and paleoclimate simulations (e.g., Wilmes *et al.*, 2019). These models yielded a relatively wide range of regional environmental conditions. Nevertheless, the patchiness of the paleobiological and geological records makes these widely accepted paleoenvironmental reconstructions questionable. Thus, elucidating the paleoenvironment is crucial for reconstructing the oceanic and atmospheric circulation or climate models (Golonka *et al.*, 1994; Goddéris *et al.*, 2014) and for understanding the past erosion or sedimentation (Salles *et al.*, 2017). Therefore, we integrated the lithofacies and foraminiferal fossil evidence via shallow stratigraphy and constructed a localised paleoenvironmental model for the late Quaternary to address this issue. We included newly acquired palaeoenvironmental information to generate a more accurate estimation of paleoshorelines. Knowledge of the local history of paleoshoreline developed in this study might improve the regional interpretation of both site and proxy records.

GEOLOGICAL SETTING

Study area

The study area is located in the district of Pontian along the west coast of Johor state in Peninsular Malaysia (Figure 1). The Quaternary coastal deposit of this area was mainly composed of peat, marine clay, and silt with different humic contents and calcareous remains (Bosch, 1988). In the western Johor coastal plain Sri Medan, shallow marine fossils occurred at an elevation of up to +15 m above the present sea level (Gray *et al.*, 1978; Tjia, 1992). These fossils represented later construct for the Quaternary deposition. Also, late Quaternary floodings at the coastal areas of Perak suggested higher palaeoshorelines at the western coast of Peninsular Malaysia compared to that of the present day (Azmi & Kamaludin, 1997). Sundaland was generally interpreted as emergent above sea level since the early Mesozoic (Hall *et al.*, 2008). Throughout the Quaternary period, this region was considered tectonically stable (Tjia, 1996), with limited data on sea-level changes from the last LGM (ca. 21 to 18 ka) until the present (e.g., Biswas, 1973; Geyh *et al.*, 1979; Tjia, 1996; Hesp *et al.*, 1998; Hanebuth *et al.*, 2000, 2002, 2004, 2011; Kamaludin, 2003; Horton *et al.*, 2005; Woodroffe & Horton, 2005; Bird *et al.*, 2007, 2010; Tjia & Sharifah Mastura, 2013; Parham *et al.*, 2014). However, several researchers disagreed with the classification of regional tectonic stability in Sundaland (e.g., Bird *et al.*, 2005; Hall, 2014), echoing the discussion of Kudrass & Schulter (1994) about the tectonic influences on sea-level changes in the Quaternary.

MATERIALS AND METHODS

Figure 1B shows the locations of BH1 (01° 23.612 N, 103° 29.118 E) and BH2 (01° 22.328 N, 103° 28.813 E) acquired using ‘Eijkelkamp peat sampler’ and ‘Mazier core barrel’ techniques. Sedimentological logging and core description (Tucker, 2003) were performed along two borehole

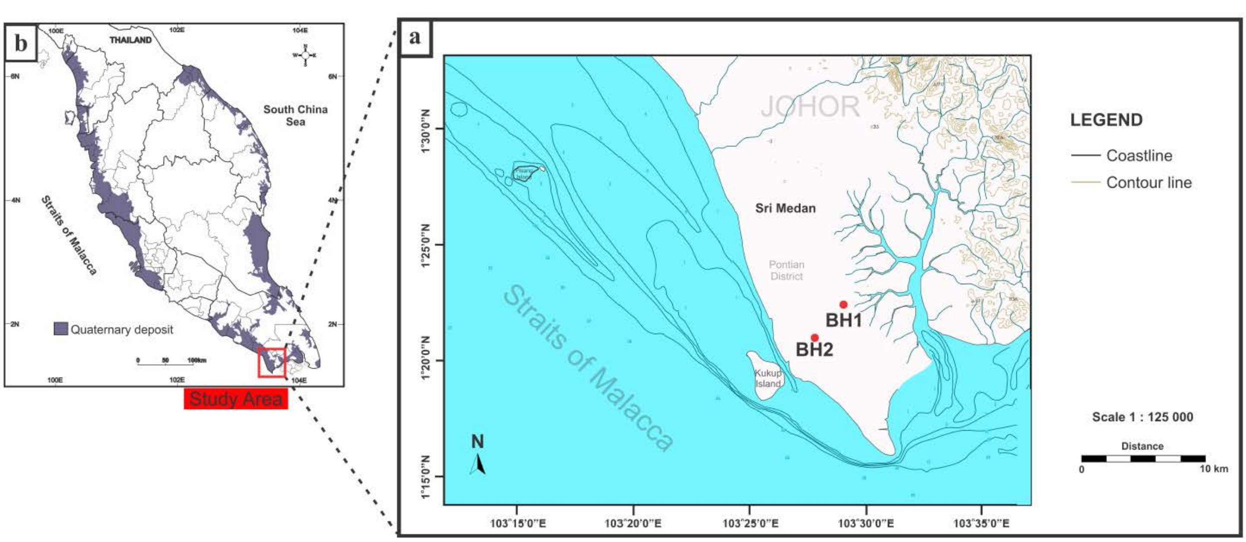

Figure 1: The study area: (A) The geographical location with boreholes (BH1 and BH2), and (B) the Quaternary coastal deposit of Peninsular Malaysia.

(core) samples (BH1 = 42 m and BH2 = 39 m) to record several parameters (e.g., colour, grain composition, and bedding features) for analysing sedimentary facies, assessing facies associations, and inferring depositional environments.

Also, micropaleontological analysis was performed with 81 sediment samples collected at each meter from the BH1 and BH2 cores. Samples were prepared by following the methods of Culver *et al.* (2012) and Minhat *et al.* (2016). Also, the foraminifera was taxonomically identified using the baseline dataset of Culver *et al.* (2012) and Minhat *et al.* (2016). Where applicable, the percentages were counted to a minimum of 300-500 individuals for each sample. Finally, the Detrended Correspondence Analysis (DCA) was performed using the software of Paleontological Statistics Software Package (PAST) version 4.04 (Hammer *et al.*, 2001) to categorise the quantitative foraminiferal counts.

RESULTS

Figure 2 shows the lithology profile of BH1 (Figure 2A) and BH2 (Figure 2B). Initial observation of a lower depth deposit (30 - 42 m) indicated the occurrence of a delta plain setting with no foraminifera. Paleosols and grey silt generally suggested the sedimentation of incised valleys and terraces (Amorosi *et al.*, 2016), while the presence of humic materials and calcareous at the interval of 23 - 30 m would imply that the site was close to land vegetation at saline conditions, possibly an estuary. Besides, calcareous fragments were absent from the upper section of the core (0 - 12 m), suggesting a correlation between the upper reaches of an estuary and the peat deposit. However, no radiocarbon dating was performed on these samples in this study. Meanwhile, Geyh *et al.* (1979) dated the deeper sediment to more than 10,000 BP. Based on the radiocarbon estimate of Geyh *et al.* (1979), this study inferred the approximate age of the core as ranging from the Late Pleistocene to Holocene. The absence of either continental or exclusively fluvial deposit further supported this inference. Thus, it was highly likely that BH1 and BH2 were accumulated during the Late Pleistocene.

FACIES ANALYSIS AND INTERPRETATION

Table 1 summarises the ten facies identified in this study via detailed sedimentological analysis, their attributes, including related processes and possible environment, and their associations. The overall profile of the facies indicated the initial deltaic or mudflat condition, followed by a rapid marine transgression with notable recurring episodes of regressions. Fluvial and terrestrial influence increased towards the top of the core, as evidenced the peat, i.e., a distinctive sign of progradation.

Facies A – Organic matter (OM)-rich clay

In this section, the clay deposit was the most predominant facies (Figure 2), which varied in thickness towards the bottom of the core from 2 to 10 m. This deposit, generally reddish to gleyed in colour, was mainly composed of OMs that included roots, leaves, and small branches in the matrix. Channelisation of structures that supported the mudflat deposition was absent. However, the high OM content of the deposit suggested that it was near the continental or marginal marine environment.

Facies B - Laminated OM-rich clay

This reddish-brown facies consisted of laminated (≤ 1 mm thick) silty clay. In the BH1 core, the thickness of the laminations increased sporadically towards the bottom of the facies. Calcareous fragments were also detected in this facies but at low abundance. At BH2, this facies was found only at the upper part of the core. The facies represented the sedimentation from low-energy flow or stagnant waters during the abandonment of channels (e.g., Miall, 1996). Fine laminae contained characteristics of delicate organic matters from terrestrial inputs. Variation of lamination thickness was associated with tidally influenced sediment structure whereby the variation originated from rhythmic ebb and tide process known as ‘tidal rhythmites’ (Tessier, 1993; Kvale, 2012). This feature was typical of a tidal flat.

Facies C - Silty clay

The greyish-dark facies comprised ungraded silty clay with sporadic calcareous sediments, and were absent in the BH2 core. In BH1, this facies occurred as gradational between adjacent fine grained-bedding, namely, facies A and D at 24 m and 33 m, respectively. Facies C was attributable to the accumulation and sediment leaching in a dry mudflat setting. The very shallow water, combined with oxidising conditions and prolonged intervals of subaerial exposure, gave rise to the facies’ colour and its variable organic contents (Plummer & Gostin, 1981; Smoot, 1983; Demicco & Gierlowski-Kordesch, 1986).

Facies D - Calcareous clay

This facies occurred in the middle section of the BH1 and BH2 cores. This ungraded facies consisted of massive reddish-brown to greyish-green silty clays with small to abundant quantities of ostracods, broken shells of bivalves and brachiopods, and echinoid spines. The layer boundary was indistinguishable from the adjacent or laminated OM-rich clay facies. Calcareous fine-grained sediment indicated the marine influence while being deposited in a tidal-influenced environment. Thus, these calcareous contents were likely carried from the inner neritic zone (Jain *et al.*, 2019). However, broken shells and brachiopods found in this sediment showed juvenile features, suggesting that this facies was estuarine sediment as the estuary was the natural breeding ground for these invertebrates.

Facies E - Mottled clays

This multi-coloured facies had a mottled appearance with generally disrupted sediment fabrics. Such appearance

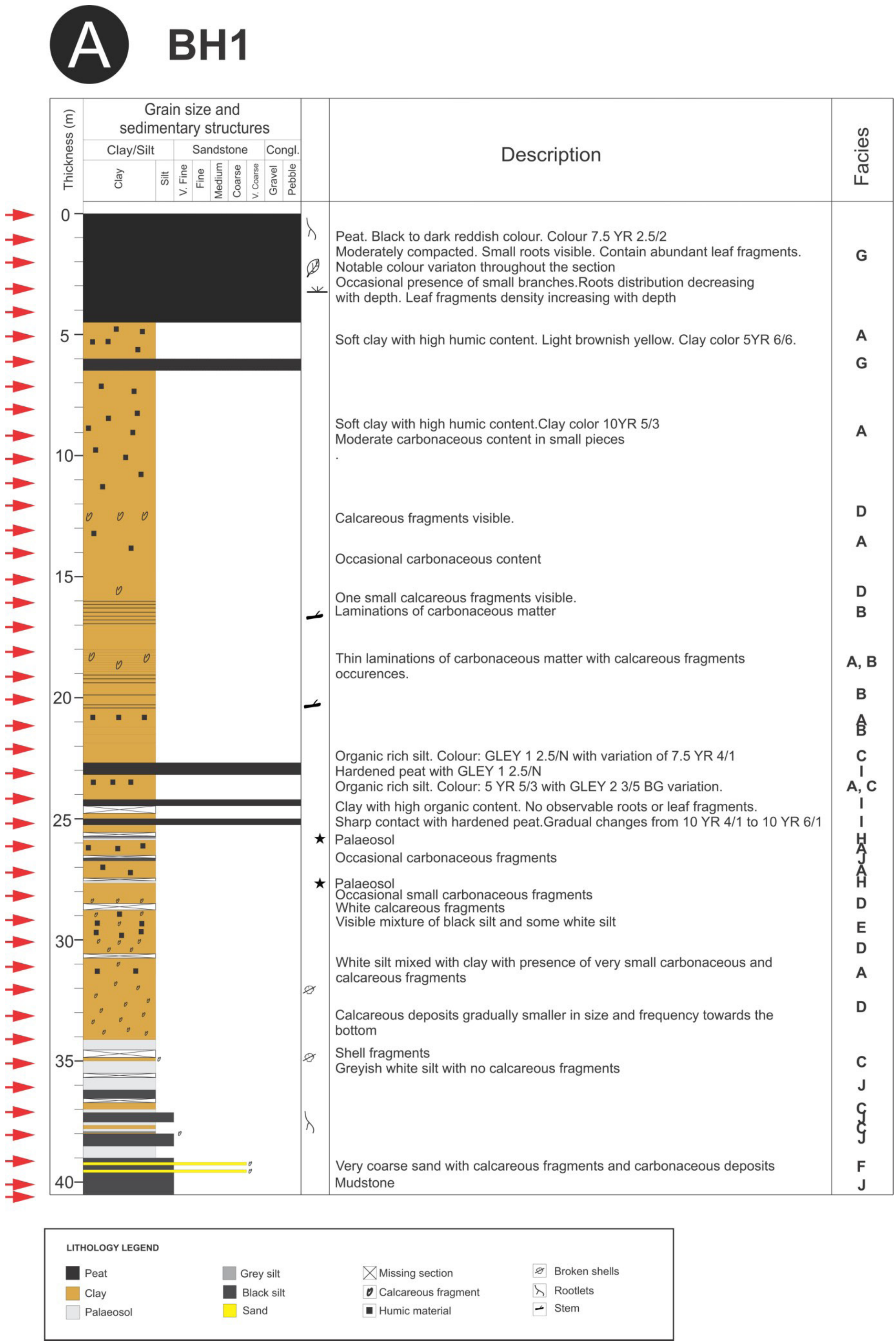

Figure 2: The identification of lithological features and facies : (A) the BH1 core and (B) the BH2 core. Remains of mollusc, foraminifera, and humic content indicated interchanges between fluvial and marine settings. Sampling points are marked by red arrows.

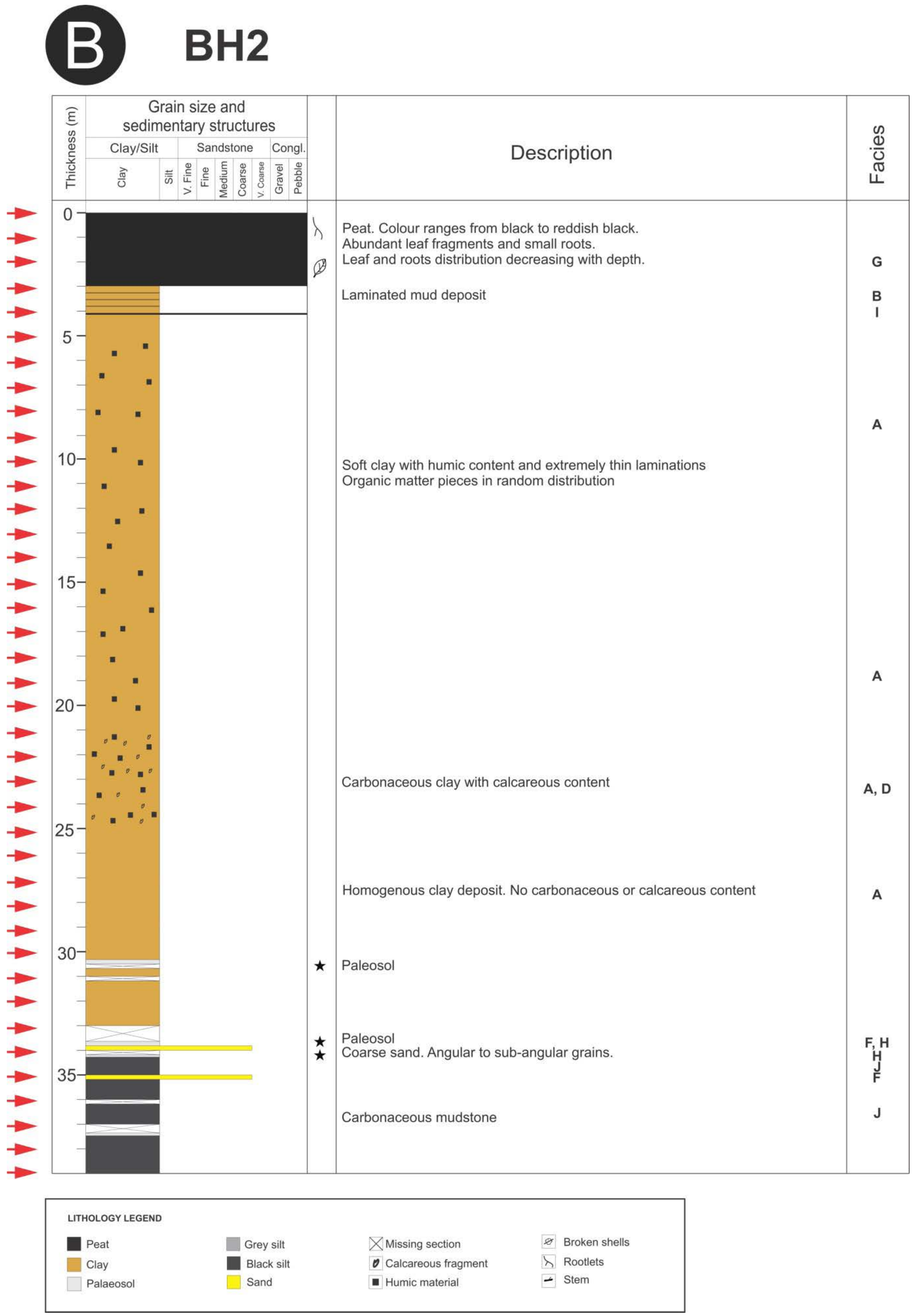

Figure 2: *continued.*

Table 1: The summarisation of facies and interpretation for BH1 and BH2.

Facies code	Facies	Characteristics	Interpretation	Depositional environment
A	OM-rich clay	Occasional rootlets and abundant carbonaceous fragments	Hemipelagic sediments in a low-energy environment	Supralittoral mudflats
B	Laminated OM-rich clay	Planar horizontal lamination	Sedimentation from low-energy flow or stagnant waters during the abandonment of channels	Tidal creek or abandoned channel
C	Silty clay	Dark to light grey	Variation in colour and organic matter content derived from different subaerial exposure rates	Dry mudflats
D	Calcareous clay	Abundant small broken shells, including juvenile brachiopods and gastropods	Pelagic or semi-pelagic sediments	Central basin to the lower estuary
E	Mottled clays	Disrupted fabrics	Fluctuation in water salinity and interaction between iron and oxygenated or reduced water condition	Middle estuary to upper estuary
F	Very coarse sands	Angular grains	Sedimentation from high energy flow	Channel-lag deposit
G	Peat	Abundant rootlets, leaves, and branches	-	Vegetated-swamp deposit
H	Paleosol	N/A	Pedogenesis or marine flooding and mineralogical components	Overbank deposit, fluvial or upper estuary
I	Hardened peat	Compacted, mixed with silt and clay	Incessant, slow-receding, moderate drainage conditions	Vegetated-swamp deposit, possibly mangrove
J	Carbonaceous mudstone	Finely fissile	Hemipelagic sediments in a low-energy environment	Deltaic, mudflats

*OM = Organic matter

suggested that the surrounding was characterised by fluctuating water impregnation and interchanging reactions of iron with oxygenated or reduced pore waters (Freytet & Verrecchia, 2002; Lindbo *et al.*, 2010). This facies occurred exclusively in BH1, suggesting that BH1 was in proximal to marine influence, which, in turn, caused BH2 to be distal.

Facies F - Very coarse sands

This facies occurred at the bottom of both cores. Its thickness ranged from 10 to 20 cm, and the thicker facies were in BH2. This facies had close contact with the adjacent mud, consisting of very coarse sand with diameters around 2 mm. These sands were angular to subangular in shape and reddish in colour. The textural immaturity of the deposit was due to mini channel lags or longitudinal braided bars of sinuous streams. Due to the inability of the transport medium to carry coarse particles, the coarser sediment would remain even after finer sediments were carried away further (Lindholm, 2012).

Facies G – Peat

This facies was marked its appearance at the upper part of BH1 and BH2, with a maximum thickness of 5 m. This reddish-to-black peat facies was composed of small roots, barks, fragments from leaves, and occasionally short branches mixed with silt to clay deposits. The peat characteristics indicated peat-forming back swamps that were poorly to moderately drained but with dense vegetation along the sinuous streams (Noorbergen *et al.*, 2018).

Facies H - Paleosol

This facies occurred at the bottom of both cores, showing sharp contact with adjacent bedding. This paleosol facies comprised white silty clay, which was fissile. Devoid of plant fragments or root traces, the paleosol indicated paleoclimatic and paleoenvironmental conditions and the duration of the exposure during the pedogenesis. However, overlying conditions due to marine flooding, the composition, and mineralogy of the underlying parent materials might also affect the paleosol features (Gustavson, 1991; Retallack, 2001).

Facies I – Hardened peat

This greyish-black facies comprised hardened peat mixed with carbonaceous silt and clay occurred at the middle of BH1 and the upper part of BH2. Its overall texture differed from facies G, as the fabrics clumped together. It was typically dull, with thicknesses varying from 10 to 25 cm. The peat beds suggested that the plant sedimentation occurred rapidly in humid paleoclimate (e.g., McCabe *et al.*, 1984; McCabe, 2009). This facies might also derive from a back swamp with persistent, slow-receding, moderate drainage, and plenty of vegetation (Diessel, 1992).

Facies J – Carbonaceous mud

At the bottom part of both cores, this structureless carbonaceous mud facies had sharp contacts, in which the mudstone was accumulated in a natural embankment or an alluvial plain (Loucks & Ruppel, 2007; Abouelresh & Slatt, 2011). However, the occurrence of carbonaceous mud indicated the more static environment of back swamps or the evacuated channels with sparse vegetation. This facies appeared more frequent in BH1 than BH2, suggesting a more dynamic environmental change in proximity to the BH1 core , associated with localised changes relative to sea level.

Facies association 1: Lower delta plain and bay-head delta

Sedimentary processes related to this facies association involved Facies C, F, and J from BH1 and Facies A, F, H, and J from BH2 (Figure 3). The first succession of facies consisted of carbonaceous mud with very coarse sand and homogeneous features. The absence of lamination suggested that deposition was in a low-energy environment with constant velocity flow. We interpreted it as a deltaic deposit consisting of overbank fines or tidal flats at the estuary's

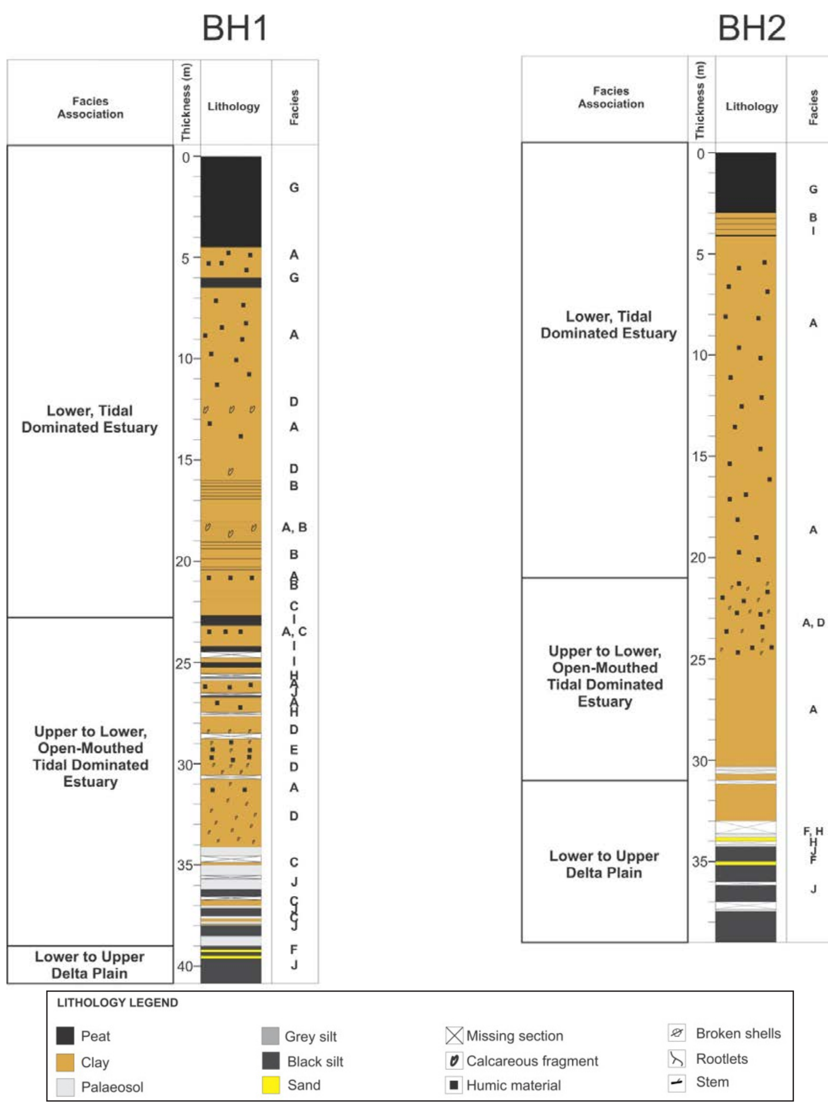

Figure 3: Facies associations of the BH1 and BH2 cores.

innermost area. The very coarse sand deposit indicated the migration and reactivation of the channel; we interpreted this as channel-lag deposits (Facies F), in which the removal of fine material through the fluvial processes caused the accumulation of relatively coarser and angular granule materials at lower flow velocities. The high organic content of the fissile mud and the oxidised silty mud represented rapid sedimentation over the poorly compacted, saturated sediments of the tidal flat in a subaerially exposed non-marine condition near vegetation. The overall trend of channelward-coarsening for this succession indicated a tide-dominated setting.

In this facies association, the bottom part of the borehole sample (~40 m) was preserved directly above the granitic basement rock. However, this association contained no marine influence or foraminifera recovery, indicating an environment with very low or no salinity. It might be attributable to the dominant freshwater influx since the subaerially exposed shelf would have a higher magnitude of fluvial influence due to the lowstand shoreline and margin (Martin *et al.*, 2011; Holbrook & Bhattacharya, 2012; Blum *et al.*, 2013). Higher freshwater influx and reduced marine influence prevented the flourishment of marine and brackish organisms. Besides, this facies association contained features related to the incised valley, such as sand deposit and silty clay (e.g., Facies F and J) that might have resulted from the lateral channel migration and resuspension of the previous channel deposit. Incised valleys originating from low relative sea level were general features in the late Quaternary (e.g., Vital *et al.*, 2010; Wang *et al.*, 2019).

Facies association 2: Upper to lower, open mouth tide-dominated estuary

Sedimentary processes related to this facies association involved Facies A, C, I, H, J, D, and E from BH1 and Facies A and D from BH2. In the second facies association, traces of OM occurred in various concentrations (Facies A, I). The OM content increased considerably in concentration when moving up of the boreholes, due probably to the estuarine deposition and a combination of autochthonous carbon sources (e.g., rootlets) and allochthonous materials from the riverine/upper estuary. In particular, mottling occurred at a depth of 30 m in BH1 due to the sedimentation of the mud over a poorly compressed, water-impregnated substrate in a setting with variable salinity (Facies E). The absence of grading in silt to clay and lamination with undifferentiated organic and calcareous deposits (Facies D) suggested the resuspension of receding and flooding flow, probably in a deltaic setting. Meanwhile, BH2 recorded mud sediment with homogeneous bedding, indicating a rapid mud deposition exposed to resuspension from the tidal current. We considered this association an interdistributary-bay deposit consisting of overbank fines or tidal flats of the estuary's innermost area.

The paleosol represented the channel incision and overbank (Facies H), while channel abandonment and progradation of the tidal-flat deposits occurred in Facies A, B, and D. Fills of tidal channels (Facies D) denoted the decreasing intensity of waning tidal flows or by channel abandonment. This avulsion might result from changes in the receding–flooding drainage triggered by storm events, as documented in the tidal channels of the Bay of Fundy (Dalrymple *et al.*, 1990, Dalrymple *et al.*, 2012). We interpreted this association as an estuary with lower and upper parts exposed to tidal influence. The abrupt lithological changes marked by hardened peat and adjacent mud deposits indicated a diverse distribution of foraminifera. The dominance of hyaline and calcareous types in foraminifera suggested highly variable environmental conditions in lateral and vertical (i.e., spatial and temporal) scales.

Facies association 3: Upper, tide-dominated estuary

Sedimentary processes related to this facies association involved Facies A, B, D, G, and I from BH1 and Facies A, B, G, and I from BH2. In the third facies association, the laminated mud with occasional calcareous contents (Facies A, B, and D) represented the sedimentation channelised by slow-moving currents in a low-energy environment with alternating conditions of slow and moderately fast flows (Facies D). The current eventually receded to an even lower flowing regime. This intercalation of OM and calcareous content in bedding with sedimentary structures of shallow water represented the mixed flats in the intertidal zone (Facies B and D). The occurrence of foraminifera in a saline environment could best be explained by tidal flooding and drainage. Besides, both peat facies (Facies G and I) recorded a maximum thickness of 5 m. Given that the peat was formed in an anoxic condition with a slow accumulation of partially decomposed OM, the obstructed oxygen flow from the atmosphere during the flooding in wetlands suggested that it was an intertidal zone.

Due to the reduced diversity of foraminifera with a calcareous test, the upper estuary changed to an environment with more variable salinity (freshwater input). Additionally, although the assemblage in the lower part of BH2 (19 - 23 m) showed a higher foraminifera diversity than those of the middle part of BH2 (19 m and higher), it was inferior in terms of the overall species count and diversity recorded in the lower estuary in the middle of BH1 core. Undifferentiated vegetation of this peat rendered the reconstruction of accumulation history highly challenging given that the appearance of a specific plant species depended largely on the geomorphic landscapes and the paleoclimate.

Facies succession

Together, facies, facies association, and biofacies suggested that Pontian generally had a marine-influenced fluvial environment, i.e., possibly incised valleys filled with fluvial sediments in an estuarine system. In particular, the lateral and vertical changes between various estuarine systems were potentially determined by the relative sea-level changes associated with the Quaternary glacio-eustasy. Also, the low-gradient geomorphological hallmarks substantially affected the sedimentation, primarily because of the paleovalley with robust correlations among the paleosol, riverine, tidal, and estuarine sediments. Correlating the lithologic units of closely located stratigraphic sections would demarcate the facies types in the Quaternary deposit in western Johor. Both borehole units were acquired from a deltaic or fluvial-estuarine, where the main litho-facies consisted of mud deposits.

The sediments were generally considered massive homogenous mud without depositional features (Shan *et al.*, 2019). This texturally homogenous mud deposit suggested the occurrence of fluid mud (MacKay & Dalrymple, 2011; Chen *et al.*, 2015), presumably due to an abundant sediment supply within the region that resulted in a highly dispersed, neutrally laminated boundary layer of mud with negligible wave actions. The high concentration of dispersed sediment within the fluid-mud bodies prevented settling, impeding the vertical segregation of sediments with unequal settling velocities (Kirby & Parker, 1983; MacKay & Dalrymple, 2011). With the tidal effect on the study site, thus, the mud sediment was exposed to the resuspension of fine-grained sediment in huge volume due to the strong bidirectional tidal current that included large mudflat intertidal exchanges.

Due to the time-velocity asymmetry of the tidal motion (e.g., Geng *et al.*, 2020; Dalrymple, 2022), the flooding would experience a higher suspension than the receding water and also in the upstream transport. First, the flooding velocities would be higher than the receding velocities but at a shorter duration. Second, the high-water slack would last longer than the low-water slack. This tidal asymmetry would be more significant upstream of many estuaries, amplifying the differences between the flooding and receding velocities and the duration of the slacking water. In turn, a short period of slacking water would allow the settling of fine-grained mud with allochthonous organic matter from various possible sources (Goni *et al.*, 2003). Indeed, the middle and higher sections of the core contained organic laminae within the mud deposit. The cyclic OM laminae implied that deposits were formed by periodic variations in the tidal-current strength (cf. Zhang *et al.*, 2017). The normal gravitational settling during short periods of slacking-water deposit gave rise to fine laminations with a lower sediment density and concentration (Ichaso & Dalrymple, 2009; MacKay & Dalrymple, 2011). The formation of these features might be attributable to the changes in both sediment supply and tidal influence with a lack of tidal resuspension at the middle/upper part of both cores. These ten facies (Table 1) were grouped into three facies associations, representing two sedimentary environments, namely, estuary and delta plain (Figure 3).

Micropaleontological analysis

Figure 4 shows the DCA with four distinct biofacies identified for each borehole (a total of eight groups) through the similarity plots of taxonomic compositions. These groups were designated Biofacies Ia to Id for BH1 and Biofacies IIa to IId for BH2. Figure 5 shows the plots of DCA with the R-mode (row mode) illustrating taxa with similar distributions across samples that were close to each other (Figure 4A). The resulting clusters A to D varied in the percentage of occurrence across the four biofacies (Figures 5A and 6B). Each biofacies was characterised by the most dominant species occurring within each cluster from A to D (Figures 5B and 6B). *Asterorotalia pulchella* occurred consistently in all biofacies, constituting 1.4% to 75.8% of the overall assemblage. More than one ecologically significant taxon with consistent occurrence was usable to name their respective biofacies.

Environmental significance of foraminiferal assemblages

In this study, 41 species of benthic foraminifera were identified (Figure 7), occurring in eight biofacies (Table 2) along the two acquired boreholes. These biofacies consisted of the following genera: *Quinqueloculina* and *Cibicidoides* (Biofacies Ia), *Quinqueloculina* and *Bolivina* (Biofacies Ib), *Asterorotalia* and *Pseudorotalia* (Biofacies Ic), *Ammonia* and *Elphidium* (Biofacies Id), *Quinqueloculina* and *Nodasoria* (Biofacies IIa), *Asterorotalia* and *Cibicidiodes* (Biofacies IIb), *Asterorotalia* and *Pseudorotalia* (Biofacies IIc), and *Ammonia* and *Elphidium* (Biofacies IId).

Most foraminiferal species found in the Quaternary deposits were generally well preserved. Foraminiferal assemblages were restricted to shallow water assemblages and subjected to marine influence. We interpreted these variations as a manifestation of paleoenvironmental changes and sea-level fluctuations. Presumably, an increment of fluvial inputs during periods of lower sea levels caused the disappearance of calcareous species, thereby reducing the foraminiferal diversity. These genera might reappear with the subsequent increment in sea levels because of a more intense marine influence. However, if an overall decrease in sea-level, albeit fluctuating, was detected in the vertical depositional trend, the calcareous taxa and species diversity would continue to decrease. Figure 3 shows consistent periods of reduced foraminiferal diversity marked by the absence of calcareous species that suggested lower sea levels. These periods were alternated with high and low foraminiferal diversities. Benthic fluctuations of species diversity might be due to the influence of tidal reworking and its magnitude during low sea levels. However, the foraminiferal diversity increased due to the tidal transportation of taxa from the inner neritic environment (Murray, 2003) deposited on the low gradient tidal flat surface through suspension settling. Thus, correlating biofacies and lithological information

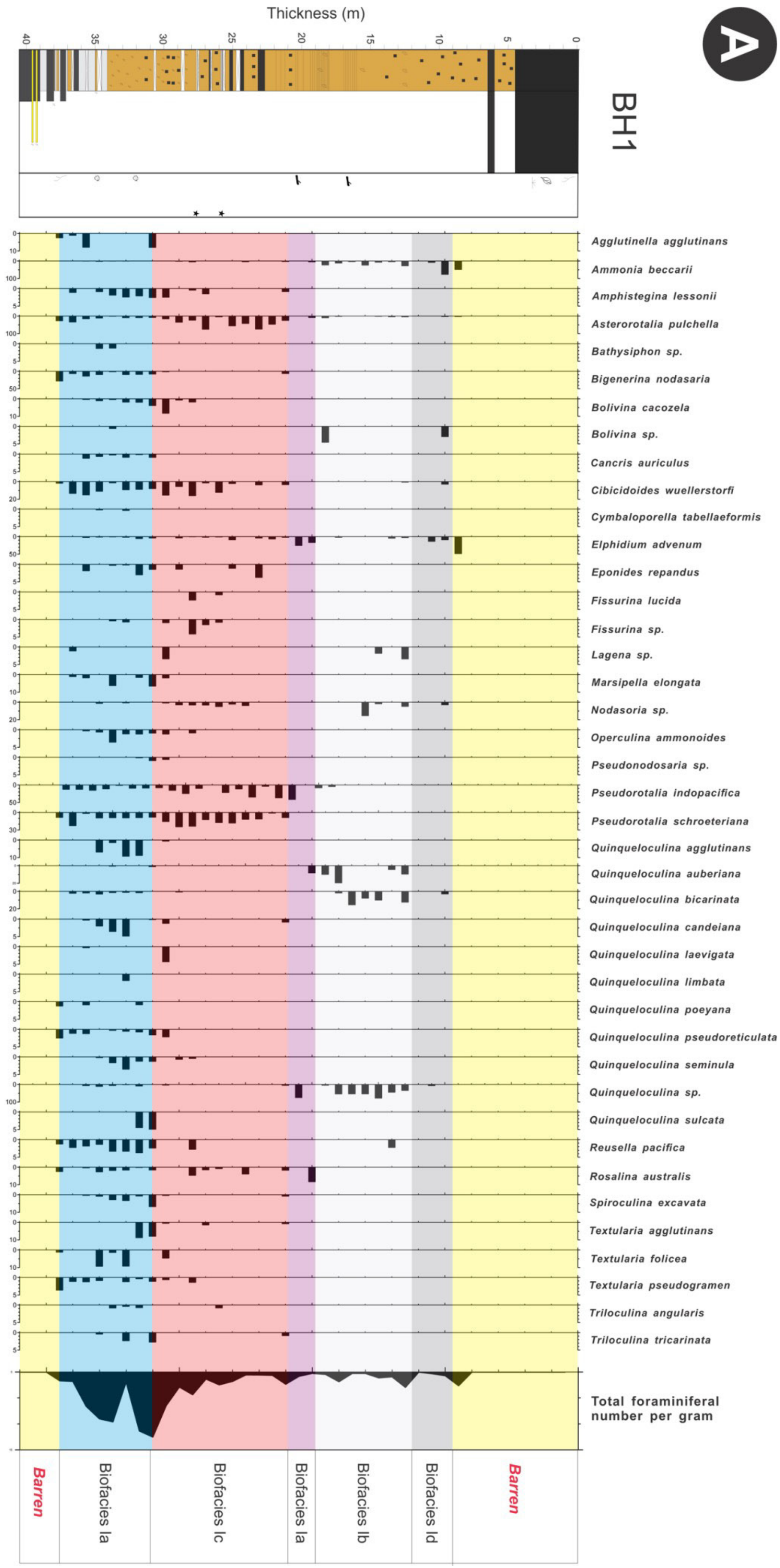

Figure 4: Foraminiferal species and their corresponding biofacies in Pontian, western Johor: (A) BH1 with higher diversity and (B) BH2 with lower diversity.

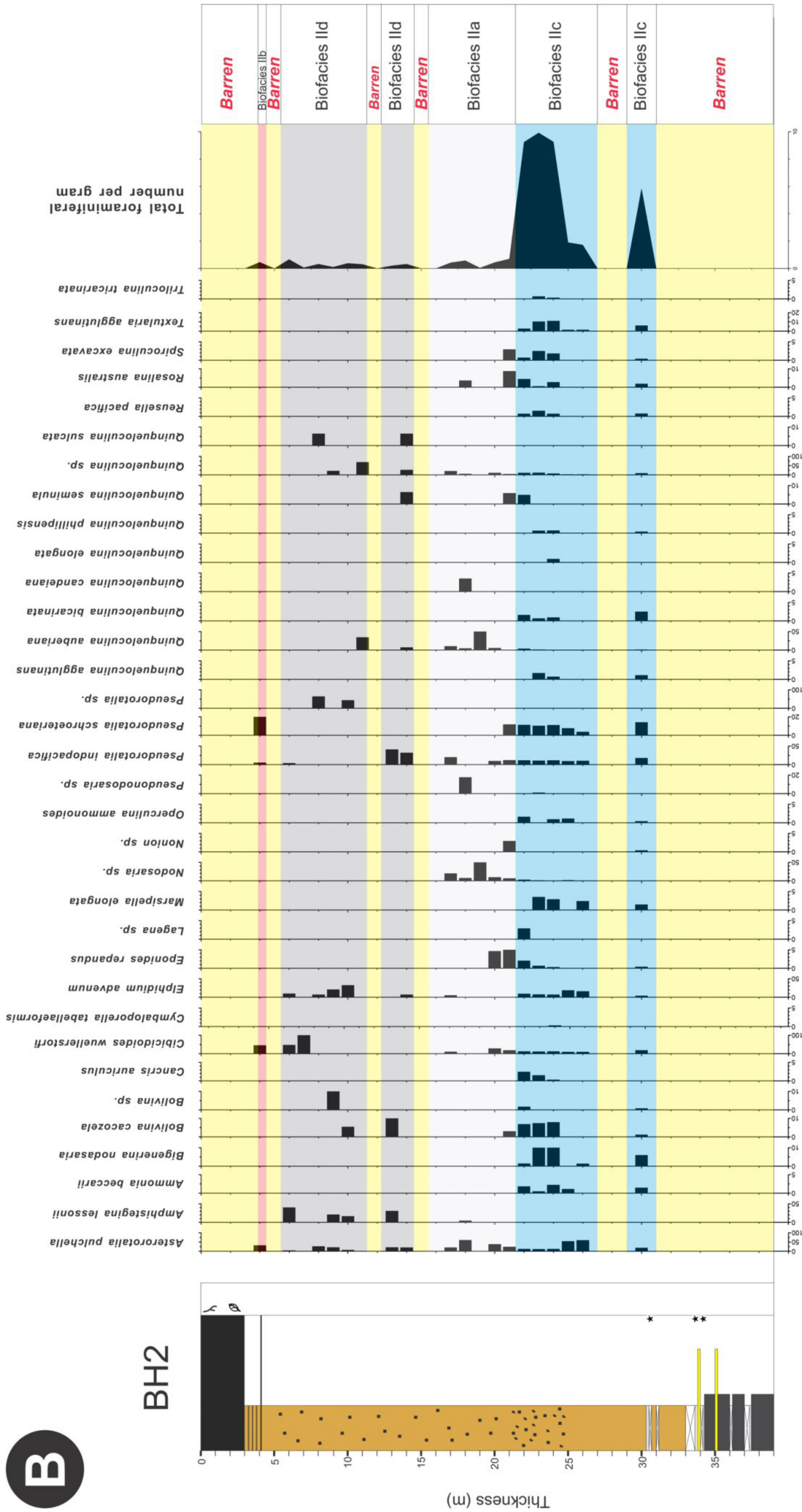

Figure 4: *Continued.*

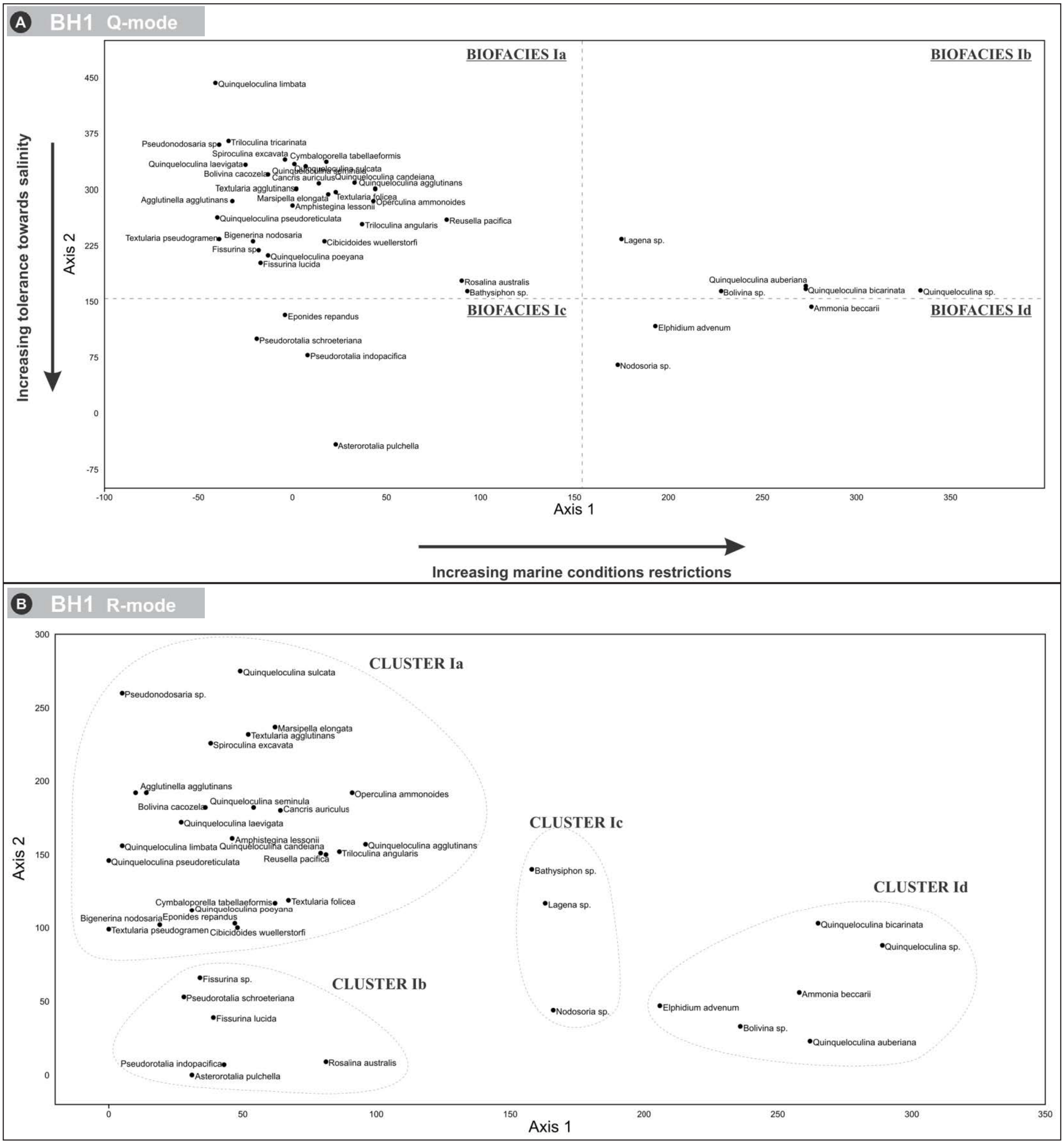

Figure 5: The DCA of BH1: (A) plot of Q-mode (column mode) delineating biofacies Ia to Id of the BH1 section at Pontian, Johor, and (B) plot of R-mode (row mode) with dashed circles encompassing various species, which represented the faunal clusters from Ia to Id.

with rapid changes in environmental conditions would allow us to identify the geomorphological origin of various species (Figure 8). In this fluvial-estuarine setting, the diversity and abundance of foraminifera served as an indirect indicator for changes in the relative sea levels in marine influence. The integrated data were subdivided further to reflect the associated sea-level changes marked as Phase I to Phase VI in Figure 8.

DISCUSSION

Implications on the reconstruction of the paleoenvironment

In this study, silt and clay-dominated sedimentary packages collected from borehole samples were mostly fluvial-estuarine deposits.These deposits might contain components from floodplain sediments deposited previously, with a clear distinction between these two sedimentation

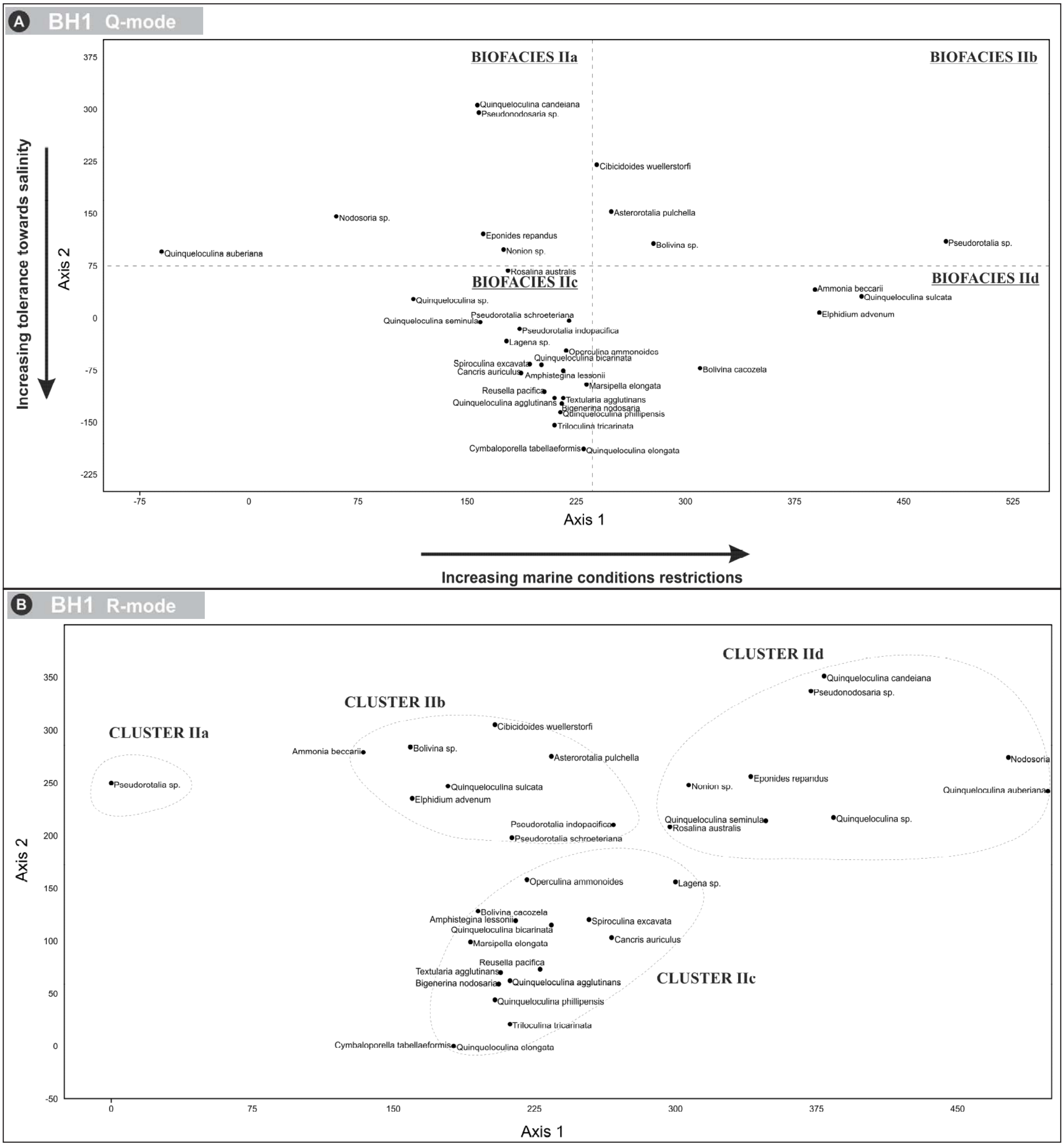

Figure 6: The DCA of BH2: (A) plot of Q-mode (column mode) delineating biofacies IIa to IId of the BH2 section at Pontian, Johor and (B) plot of R-mode (row mode) with dashed circles encompassing various species, which represented the faunal clusters from IIa to IId.

conditions based on the carbonaceous mudstone (Facies J) and the underlying clay deposit (Facies A, B, C, and D). This study proposed a model of a single estuarine system for the stratigraphical correlation of BH1 and BH2, in which BH1 comprised proximal marine segments, and BH2 had more fluvial-influenced segments. Thus, BH1 was pivotal in determining the oceanic influence as it was more proximal to the shoreline with foraminiferal assemblages correlated to the relative sea-level fluctuations. This system began with the establishment of a small tidal-dominated riverine basin in the flooded paleovalley (Figure 8 and Biofacies Ia - Id) and a peat-forming estuarine channel that resulted in the flooding of a supratidal zone (Figure 8 and Facies G). Figure 7 summarises the paleoenvironment and relative sea level in the study area from Pontian, Johor (Figure 9), which was divisible into six phases:

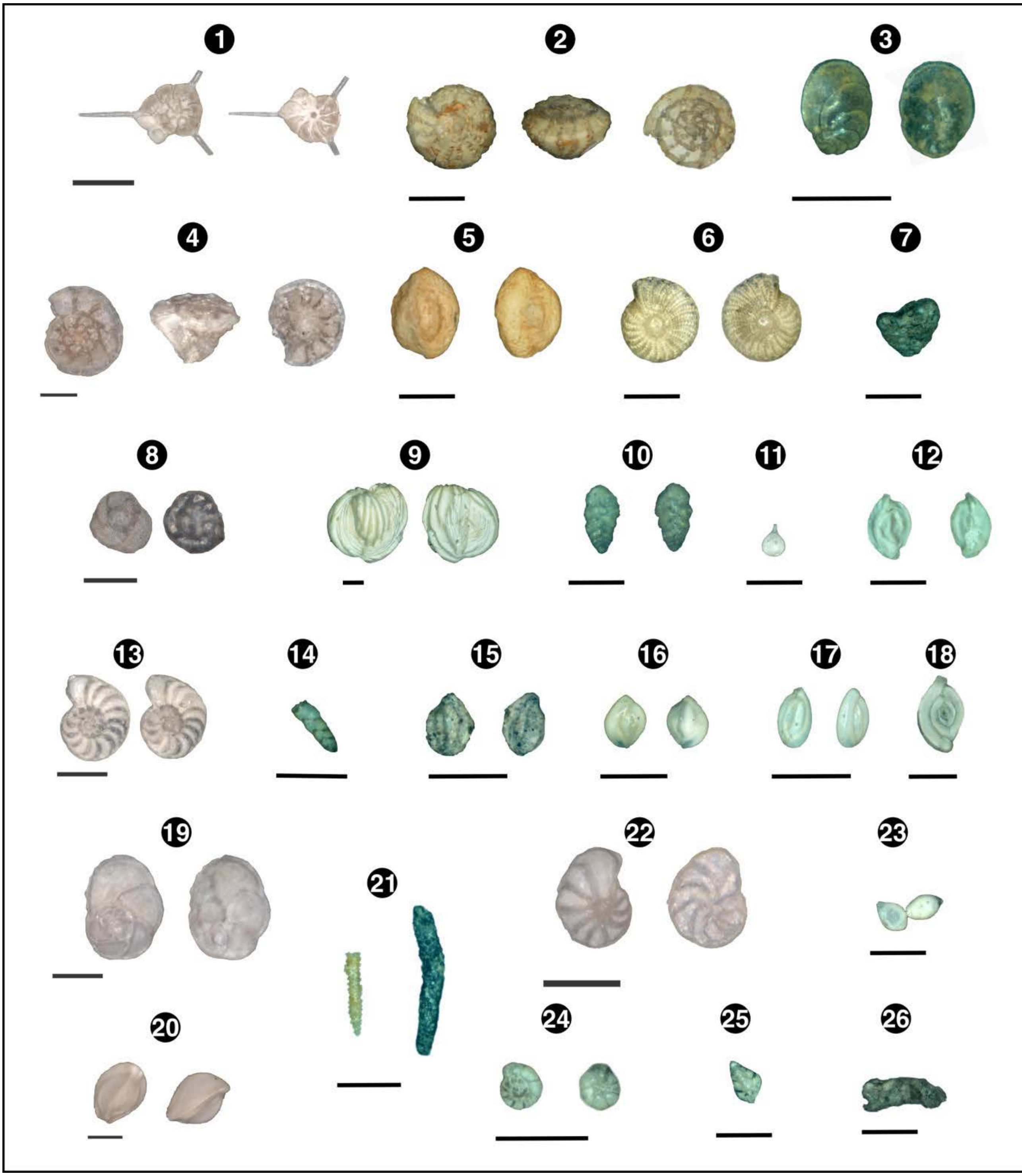

Figure 7: Microphotographs of some foraminiferal species identified in this study. 1-*Asterorotalia pulchella*; 2-*Pseudorotalia indopacifica*; 3-*Cancris auriculus*; 4-*Pseudorotalia schroetiana*, 5-*Quinqueloculina philippinensis*; 6-*Elphidium advenum*; 7-*Textularia pseudogramen*; 8-*Rosalina globularis*; 9-*Quinqueloculina* sp.; 10-*Textularia agglutinans*; 11-*Lagena* sp.; 12-*Quinqueloculina sulcata*; 13-*Operculina ammonoides*; 14-*Bolivina* sp.; 15-*Quinqueloculina agglutinans*; 16-*Quinqueloculina auberiana*; 17-*Quinqueloculina seminula*; 18-*Spiroculina excavata*; 19-*Eponides repandus*; 20-*Triloculina tricarinata*; 21-*Marsipella* sp.; 22-*Cibicidoides* sp. 1; 23-*Fissurina* sp.; 24-*Ammonia beccarii*, 25-*Reusella pacifica*, and 26-*Bigerina nodasaria*. The scale bar represents 500 microns (0.5 mm).

Table 2: The foraminiferal assemblage and their inferred depositional environments.

Core	Biofacies	Section Thickness (m)	Assemblage Characteristic	Environmental Range
BH1	Ia	31 - 38, 19 - 21	*Quinqueloculina – Cibicidoides*	Open coast – inner/middle neritic
	Ib	12 - 19	*Quinqueloculina – Bolivina*	Coastal to estuary/bay
	Ic	21 - 31	*Asterorotalia - Pseudorotalia*	Estuary with variable salinity
	Id	9 - 12	*Ammonia - Elphidium*	Restricted conditions
BH2	IIa	16 - 22	*Quinqueloculina – Nodasoria*	Coastal to estuary/bay
	IIb	4 - 5	*Asterorotalia – Cibicidiodes*	Coastal to estuary/bay
	IIc	22 – 27, 29 - 31	*Asterorotalia – Pseudorotalia*	Open coast – inner/middle neritic
	IId	6 – 11, 13 - 14	*Ammonia - Elphidium*	Restricted conditions

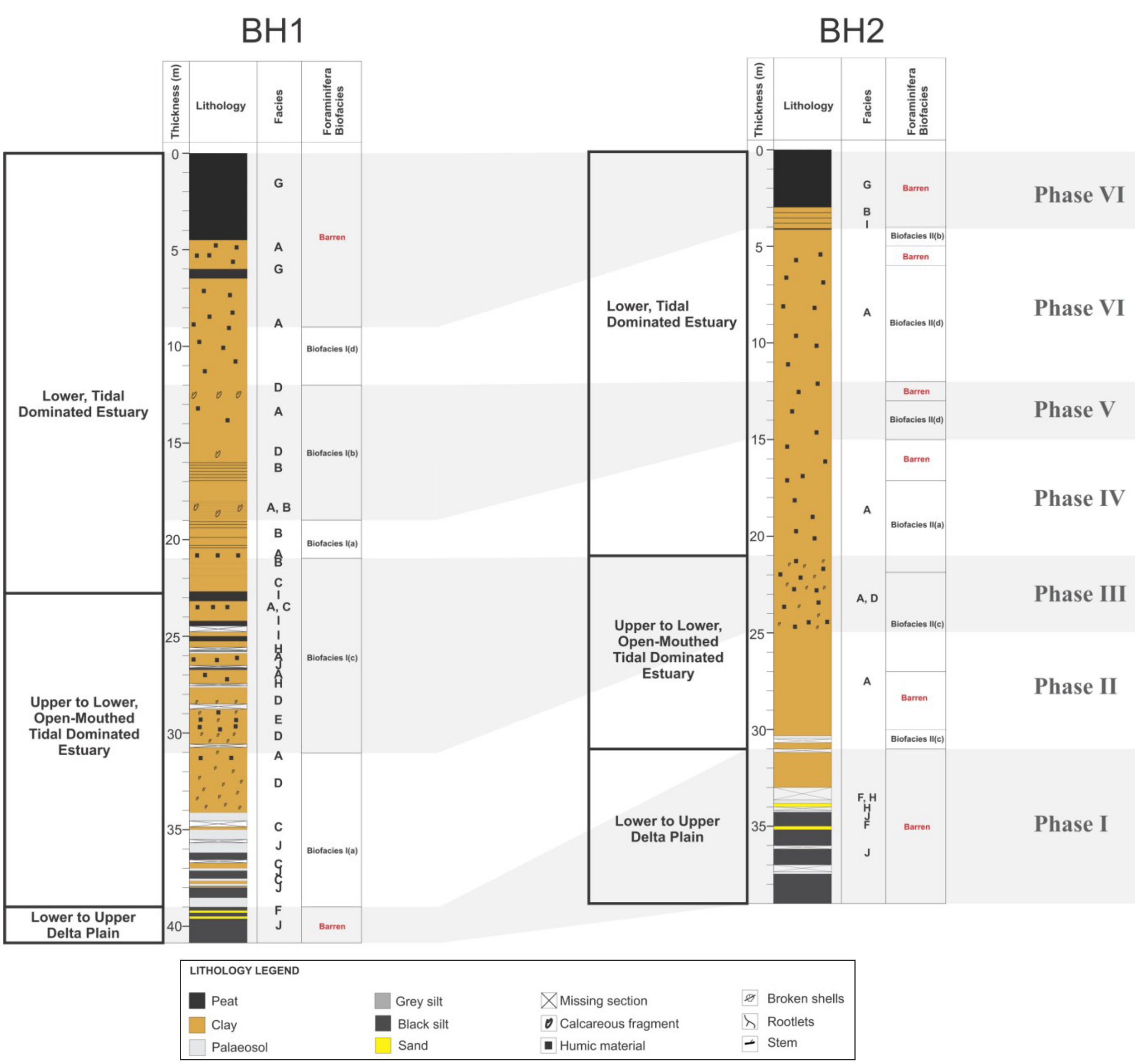

Figure 8: Correlation of BH1 and BH2 based on sedimentology and foraminiferal analysis with different subdivisions from Phase I to Phase IV.

a) Regression (Phase I) – channel incision and sedimentation of channel lag and flood-plain deposits.
b) Transgression or intrusion (Phase II) – the formation of funnel-bay estuary and sedimentation of floodplain deposits.
c) Regression (Phase III) – exposure and weathering of fluvial and tidal sediment. Possible rejuvenation of small channels and down-cutting due to paleosol formation.
d) Regression (Phase IV) – draining the bay formed a tidal creek on the flood plain.
e) Regression (Phase V) – development of the supratidal zone with vegetations cause the formation of the peat deposit, and
f) Regression (Phase VI) –the development of mangroves and a combination with previous peat deposits (retrogradation) caused the draining of the bay.

Relative sea-level changes from Phase I to Phase VI in the subdivision of Figure 6 were estimated as localised to a basin-scale (Figure 9). For Phase 1 (Figure 9A), a non-marine depositional system initially underwent a significant configuration during the Late Pleistocene, based on the estimation in response to sea-level changes. Subaerially exposed mudflat with varying carbonaceous content (Facies J) and very coarse sandy channel-lag deposit (Facies F) supported the interpretation for this succession. At this phase, the absence of foraminifera in both boreholes suggested a lack of marine influence, i.e., at lower sea levels. The regression-induced low sea level was most likely sustained due to the oxidising sediment and lateral channel migration as part of the low-gradient intertidal system. However, there was no age control on the timing of regression and associated valley incision. Also, vegetation features such as roots and leaf fragments were absent, probably because the vegetation cover of a particular species was not dense enough to prevent erosion and the formation of a large-scale system (Bosch, 1988). A similar sedimentation pattern for BH1 and BH2 at this succession highly corroborated a widespread dendritic network of tidal creeks traversing an estimated distance of 4 km between these two cores.

Also, the ensuing transgression had significantly afforded the initial filling of the paleo-valley with tide-dominated estuarine sediments (Figure 9B, Phase II), which were mostly attributable to Biofacies 1c. For the increment of sea level after a lowstand period, the transgression and marine flooding inevitably happened to the incised valley formed during the recession of sea level (Catuneanu *et al.*, 2009). The marine flooding contained abundant foraminifera that indicated coastal to open marine conditions (i.e., Biofacies Ic, 1d). Meanwhile, the floodplain facies with low organic content (Facies J) suggested a moderate to high adaptation to the geomorphic influence imposed by the rapid rise of the relative sea level. Such an increment was most likely due to the global sea-level rise (Last Glacial Maximum) during the Late Quaternary.

Moreover, the geomorphology might have transformed into a funnel bay or lagoon estuary during the regressive cycle (Figure 9C, Phase III) based on the foraminiferal assemblage from Biofacies I(d) with limited diversity in an environment of high salinity. Presumably, the funnel bay-lagoon took place, similar to that of Culver *et al.* (2012), in a highly saline marine environment that reflected the sedimentation of the lagoonal setting brought by periodic tidal currents. High flow velocities at the flood tide would move the coarser material seawards. Consequently, sand deposits could be reworked into tidal bars. Besides, differentiated bedding, such as lamination and clear grain size sorting, were limited, indicating a large volume of sediment discharge coupled with the constant reworking of fine material throughout the normal tidal cycle. With a sufficient sediment supply to sustain the net seaward sediment transport, thus the landscape configuration had significantly changed, laterally and vertically, throughout this phase. The reshaping of the previously flooded valley might have also taken place due to progradation, but the evidence of a restricted bay was vague.

The recurrence of a paleosol and hardened peat with silty components suggested the occurrence of regression in the second phase (Figure 9D, Phase IV). The paleosol had been chemically weathered with leached sediment colour, indicating oscillations between wet and dry climates. The hardened peat was very dark in colour, visually resembling charcoal. However, such a dark colouration was probably related to the Quaternary forest fire in the Sunda shelf (*cf.* Taylor *et al.*, 1999). Meanwhile, Biofacies Ia and Ib, OM-rich clay (Facies A), and silty clay (Facies C) supported the scenario of a small stream network with low marine (tidal) influence. With a higher terrestrial impact, as indicated by the carbonaceous input and increasingly fluvial condition, the foraminifera with low diversity (Biofacies Ia and Ib) could tolerate low salinity settings. The fluctuating fluvial-flow magnitude was due to the tidal influence within the tidal-fluvial transition zone (Van den Berg *et al.*, 2007). Therefore, an alternation of dry and wet climate settings was implicated throughout this regressive phase.

The succession consisting of Facies A and Facies B biofacies was dominated by a subsequent regressive cycle (Figure 9E, Phase V), in which the lateral migration of fluvial channel near vegetation indirectly laminated the clay deposit. The succession of the top section contained no foraminifera, suggesting a lower sea level free from marine influence. The occasional deposition of calcareous clay might be attributable to the sediment transport during the king-tide period and was closely related to the migration of sinuous channels during the lowstand within this partially inactive delta plain. This migration encompassed abandoned distributary channels prone to strong fluvial influence and reduced river discharge reworked by tidal currents (Dalrymple, 2006).

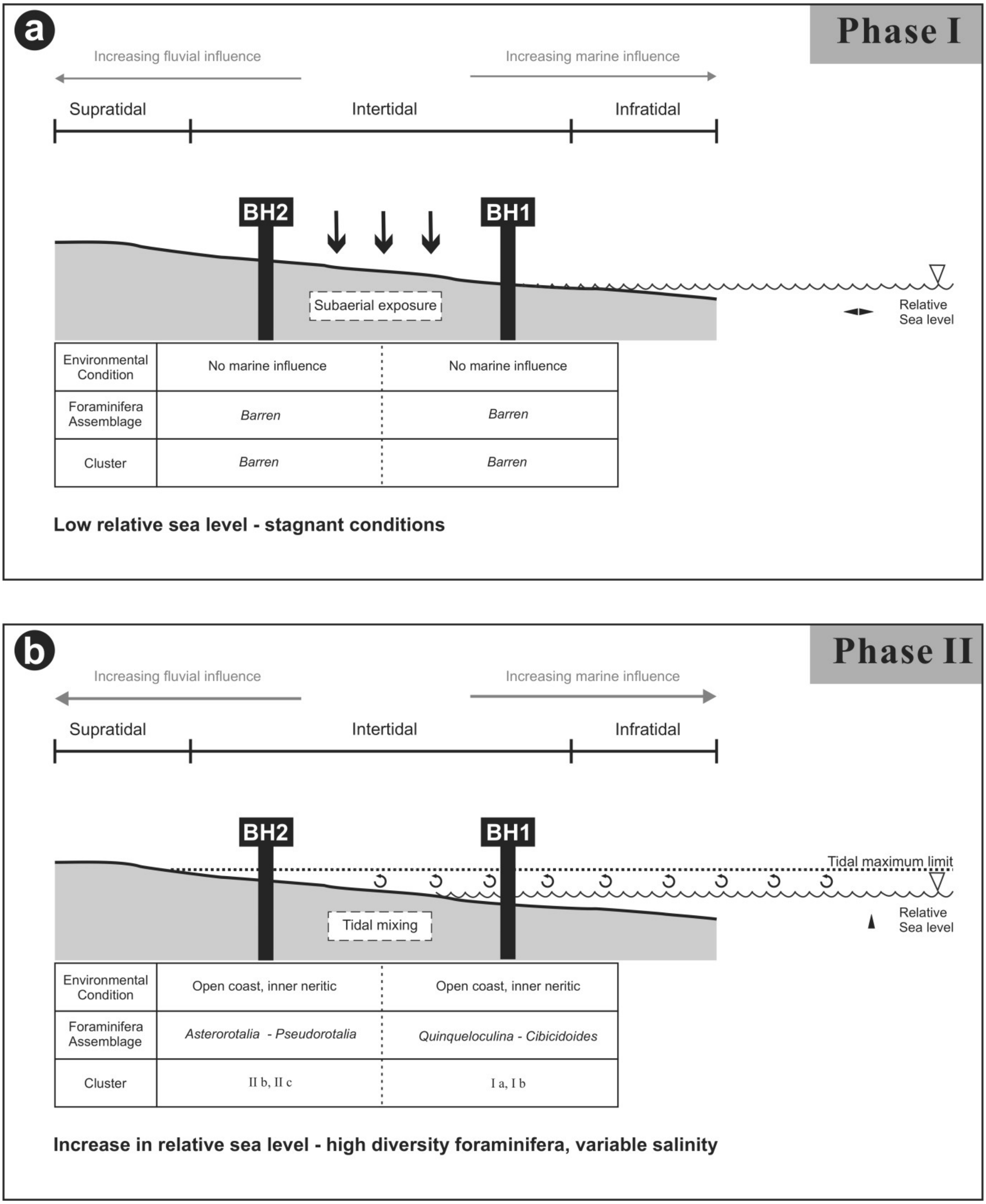

Figure 9: The proposed paleoenvironment and factors influencing their classification, the relative importance of changes in the relative sea level, tidal range, and sediment supply (Phase I to Phase VI).

The subsequent development of peat succession (Facies G) was most likely attributable to a relatively consistent sea level with a high sediment supply (Figure 9F, Phase VI). The sedimentation rate might outpace the accommodation space provided by the low-gradient floodplain, thereby prograding the previous bay. Meanwhile, the slow-moving fluvial setting encouraged the growth of vegetation, which eventually established a vertically extensive peat succession at the top of the BH1 core.

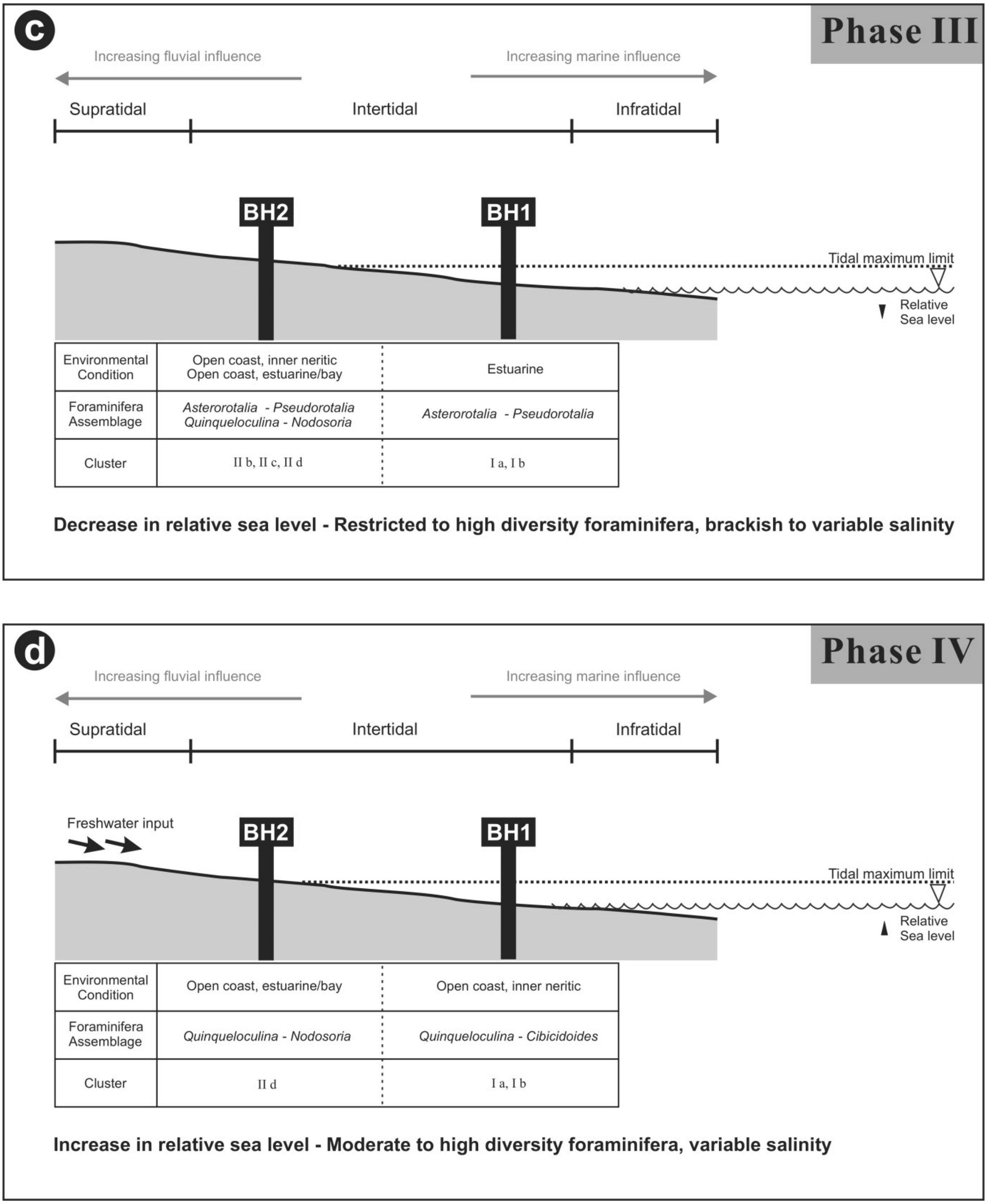

Figure 9: *continued.*

Implication on the paleoshoreline

This study reconstructed the paleoenvironment of Pontian to demarcate its Quaternary shoreline. At present, Pontian has a very gentle slope of terrain features with little changes in elevation over a relatively long distance (> 20 km). Hence, we could infer that the low-gradient streams and rivers occurred regionally and meandered through extensive valleys. In this respect, the combined flow and sediment transport in meander bends showed bedload and suspended load charted separate paths (Dietrich & Smith, 1984). Specifically, the bedload was transported towards the outer bank downstream of the bar

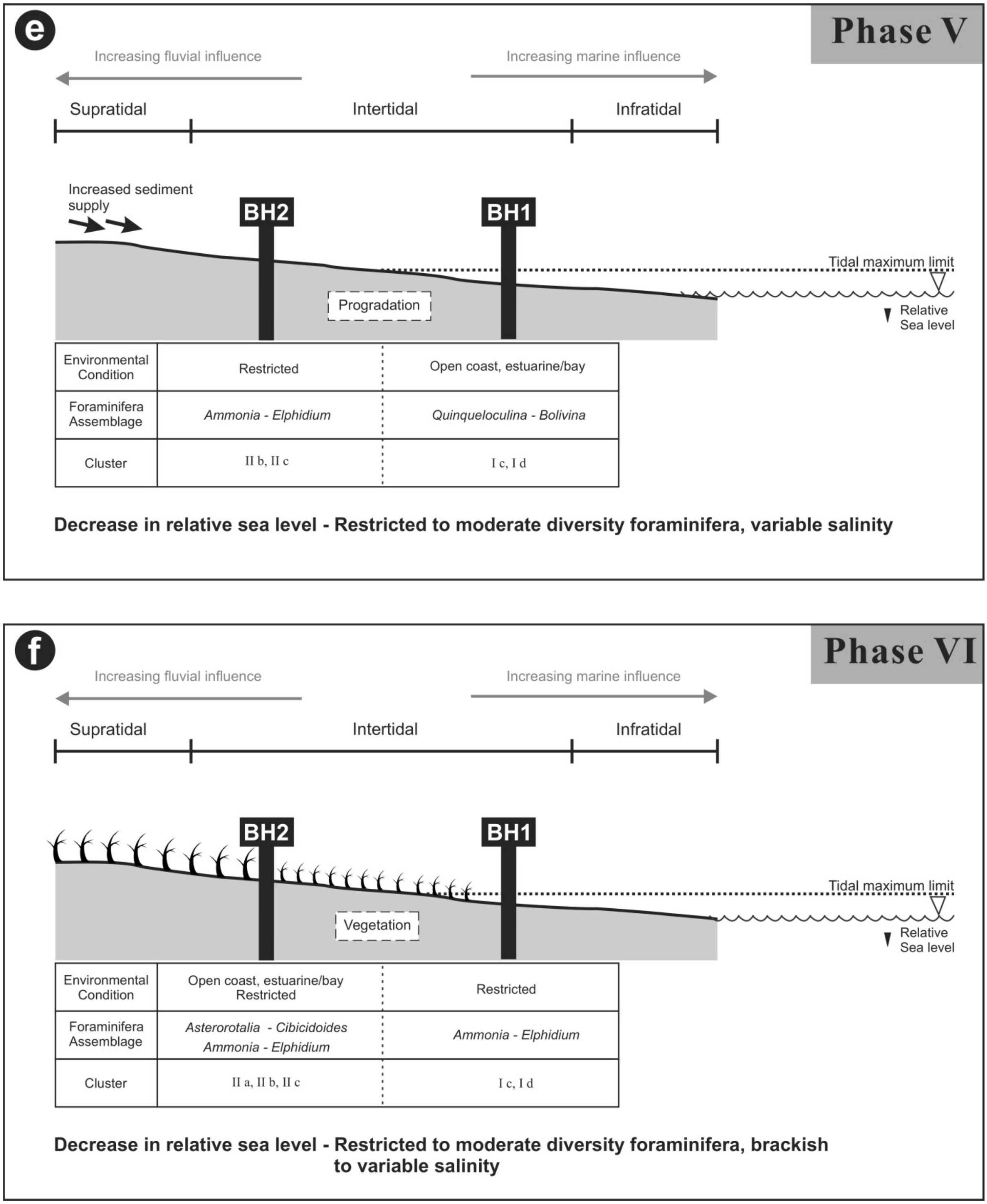

Figure 9: *continued.*

apex, while the suspended sediment was towards the bar (Dietrich & Smith, 1984), giving rise to fine bars at the downstream end (Nanson, 1980; Clayton & Pitlick, 2008). The change in salinity suggested a moderate-to-strong nonlinear response of a low-gradient estuarine system to the sea-level rise (Mulamba *et al.*, 2019). Incidentally, this study showed that sedimentation conditions in the Quaternary were linked tightly to the relative changes in the sea level. A similar scenario occurred in the wide terrestrial area of Keriang area, Kedah, on the west coast of Peninsular Malaysia due to exposure to extensive fall in the sea level (Khoo, 1996).

For western Johor, only one record showed the occurrence of sand ridges in the past along the present shoreline, i.e., at the east of Batu Pahat granite (Bosch, 1988). The occurrence of past sand ridges along the current shoreline was interpreted as the result of the maximum transgression of the relative sea level (Mallinson *et al.*, 2014; Parham, 2016). However, the term 'sand beach' inherently refers to wave-induced deposits (Jiang *et al.*, 2015; Gallop *et al.*, 2020), whereas the lower part of west Peninsular Malaysia is a sheltered tidal-dominated coast. Thus, simplified direct interpretation of paleoshoreline at the point of the sand ridges may not be entirely accurate because the distribution of sands was limited in a tidal-dominated environment with many possible interactions. Examples of potential complex interactions in shallow marine involving sandy deposits included sand ridges and bar deposits that occurred as estuarine or deltaic-distributary mouth bars (Dalrymple *et al.*, 2003). Besides, sand ridges might be related to tidal bars in estuarine systems (Leuven *et al.*, 2016), while the landward migration of sand ridges related to sea-level rise with the establishment of 'quasi-active sand ridges' (Liu *et al.*, 2007) from the tidal current using recycled sand materials. Based on the degree of wave exposure (Daidu *et al.*, 2013), morphodynamics (Short, 1991), and topobathymetry (Genchi, 2020), the tidal-dominated environment was classifiable into various supplementary groupings. Thus, lithological profiling alone could not be a definitive criterion for demarcating the past shorelines, especially for the west coast of Peninsular Malaysia, which was under tidal influence.

Figure 10 shows the morphological indicators (coastal landforms, such as mangroves and tidal plains) and shallow stratigraphy in this study to estimate the paleoshoreline in western Johor. While this study area is presently sheltered from direct wave influence from adjacent seas (the Indian Ocean and the South China Sea), the tidal force significantly affected the distance and direction of salt marsh-mangrove boundaries in the past (Peterson & Bell, 2012, 2015). This study presumed the dispersal of mangroves in this tidal-dominated estuary setting at Sungai Pulai, which was subjected to the receding and flooding of the tidal force. Using the boundary classification of Figure 8A (Hasmadi *et al.*, 2011), we estimated the terrestrial boundary of mangroves as the maximum limit of tidal influence. Thus, the observed tidal range limit was transcribed as the paleoshoreline, while the positioning of peat-forming mangroves served as sea-level markers (Scholl & Stuiver, 1967; Khan *et al.*, 2017) provided that it was limited to and exclusively found at the upper part of the intertidal zone (Davis, 1940; Davis & FitzGerald, 2009). A similar estimation of relative sea-level positions could be derived from the lithological profile and analysis of the depositional environment (Hanebuth *et al.*, 2000; Barnett & Harvey, 2001).

In the present study, the paleoshoreline was estimated from cores with a progressive description of sedimentary facies on microfossil assemblages that defined the coastal environment. In contrast, previous estimations on the Quarternary paleoshoreline position were very weakly constrained by direct observations and were entirely dependent on the available surface sediment. The

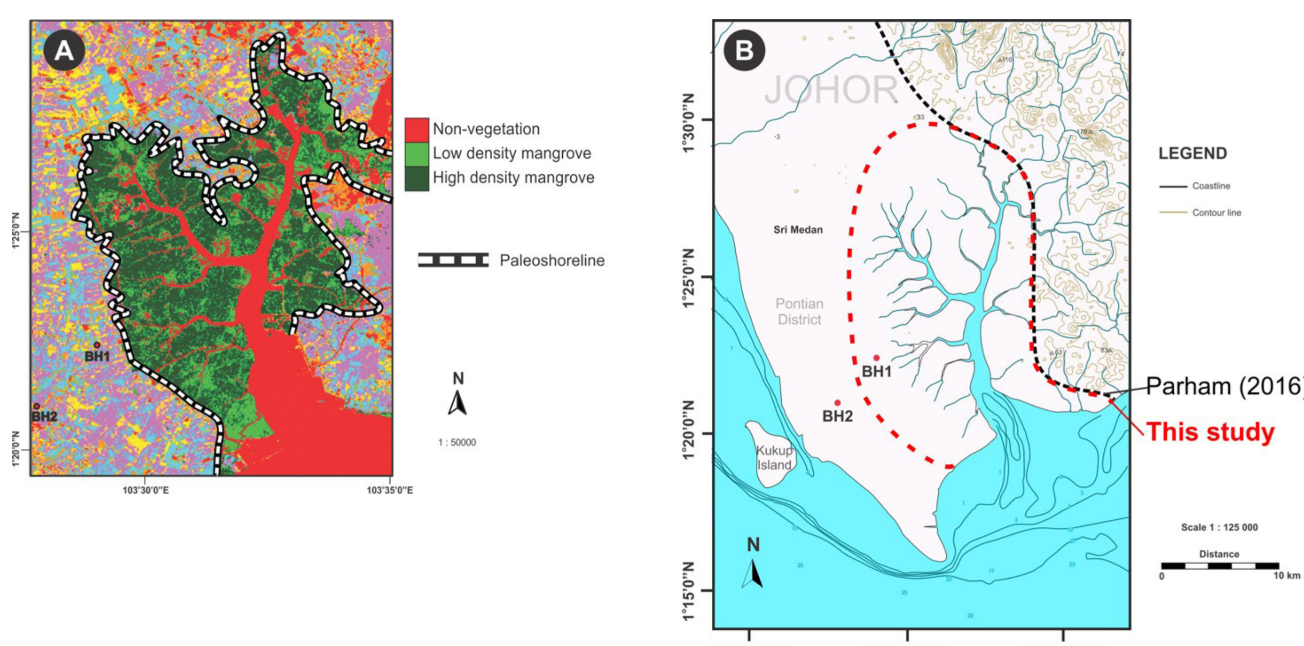

Figure 10: The integration of morphological indicators and shallow stratigraphy for the estimation of the paleoshoreline in western Johor in this study: (A) the estimated maximum paleoshoreline using the surface boundary classification map modified from Hasmadi *et al*. (2011) and (B) a comparison of paleoshorelines between the present and previous studies.

paleoshoreline estimated by Parham (2016) would imply that Quaternary sediments were mapped in a geological context (Bosch, 1989) and soil survey (Law, 1970) of Peninsular Malaysia, i.e., deposited in a marginal or shallow marine environment. However, one may argue that detailed data supporting such estimation in the area are lacking. In contrast, this study found a few episodes of flooding events indicated by the foraminiferal data, implying several migrations of paleoshoreline throughout the sequence, including the configuration of the maximum paleoshoreline (Figure 10B). However, our proposed paleoenvironmental model did not estimate the actual age and timing of each paleoshoreline position because radiocarbon dating analyses were not performed in this study.

Based on several cohort studies, further depositional age constraints could be placed on the base of peat succession at the upper part of both boreholes in this study. For example, a thick sequence of peat deposits yielded an age of approximately 7,000 BP (Geyh *et al.*, 1979). Besides, within the Asia-Pacific region, relatively high sea levels were recorded at approximately 6500 cal BP and 4000 cal BP, and relatively low sea levels at 5000 cal BP and 2000 cal BP (Sinsakul *et al.*, 1985; Sinsakul, 1992; Tjia, 1996; Fujimoto *et al.*, 1996, 1999a). Also, the relative sea-level variation, which was predominantly attributed to climate variations, might have consequently provided space for the accumulation of OM during the regressive phase. Meanwhile, across the Straits of Malacca, the development of a peat swamp forest at Siak River in Sumatera, Indonesia took place between 6000 and 5000 BP (Supardi & Neuzil, 1993; Fujimoto *et al.*, 2019), and this peat swamp forest might have expanded rapidly between 4000 and 2000 cal BP (Fujimoto *et al.*, 2019). Together, these findings provide an approximate age window from 7000 to 6500 cal BP to present for the peat development in western Johor. However, the relative sea level in Pontian seemed to be slowly declining since 6500 BP as mangroves could only survive at the rising sea-level rate lower than 7 mm per year (Saintilan *et al.*, 2020). Hashim *et al*. (2022) investigated the clay mineralogy of the BH1 core to determine the correlation between paleoclimatic changes and radiocarbon ages estimated by Geyh *et al*. (1979). We extended the similar correlation for BH1 and BH2 core data using the same age constraint (Figure 11).

The relative sea-level estimation in Pontian of Johor seemed to resemble the sea level during the late Quaternary (e.g., Hanebuth & Statteggar, 2004). Using palynology as a sea-level indicator on coastal deposits during the Quaternary, Kamaludin (1993) concluded that the progradation and development of the coastal plain at Kuala Kurau were attributable to the interactions among transgression, regression, and sediment deposition during the Holocene. Meanwhile, Klang and Kuantan showed a higher sea level in the mid-Holocene (Kamaludin, 2002), which was similar to the sea level in Peninsular Malaysia during the Quaternary. Tjia (2004) and Tjia & Sharifah Mastura (2013) reiterated this view on the prograding coastline in many areas (e.g., Sungai Muda, Kedah, and Sri Medan, Johor), which was attributable to relatively low wave energy and abundant sediment supply, similar to the findings of this study.

CONCLUSION

The major transgression event of the Late Quaternary sea resulted in the progradation of estuarine sediments over deltaic sediments in the study area, Pontian, Johor, which showed a close relationship between coastal environments and sub-environments of deposition with its corresponding relative sea-level positioning. Thus, the investigation and model development of the Quaternary deposits should encompass the determination of specific environmental settings. Differentiating the depositional environment from its sub-environments would help clarify problems in distinguishing paleoshoreline positions. Since the paleoshoreline migration was often described based on the broad usage of terms, such as “major flooding” during the Late Quaternary, thus determining the facies within the Quaternary deposit of this region would recognise facies within coastal, even in sections without bedding dissimilarity. Information from this study further refined the foraminiferal records of South East Asia. Sedimentary and foraminiferal evidence showed that the current shorelines might have significantly submerged for a certain period. Fluctuating sea levels during the late Quaternary were relative to some changes in the chronostratigraphic background. Different datasets and investigations on various sites would be necessary for future studies.

ACKNOWLEDGEMENTS

This study was partially supported by a grant from the Higher Education Ministry of Malaysia (FRGS/1/2013/STWN06/UKM/02/1). We thank the anonymous reviewers for their valuable comments and insightful review of our manuscript. We sincerely appreciate their time and effort, which helped us in improving the quality of the manuscript.

AUTHOR CONTRIBUTIONS

AHH conceptualized the original idea and discussed it with HJ and RO. All authors agreed with the main objective and idea of this paper. Laboratory analysis were performed by AHH. Main section of the manunscript was written by AHH and further elaborated by HJ and RO. Resources and funding were provided by HJ and RO.

CONFLICT OF INTEREST

The authors declare there is no conflict of interest.

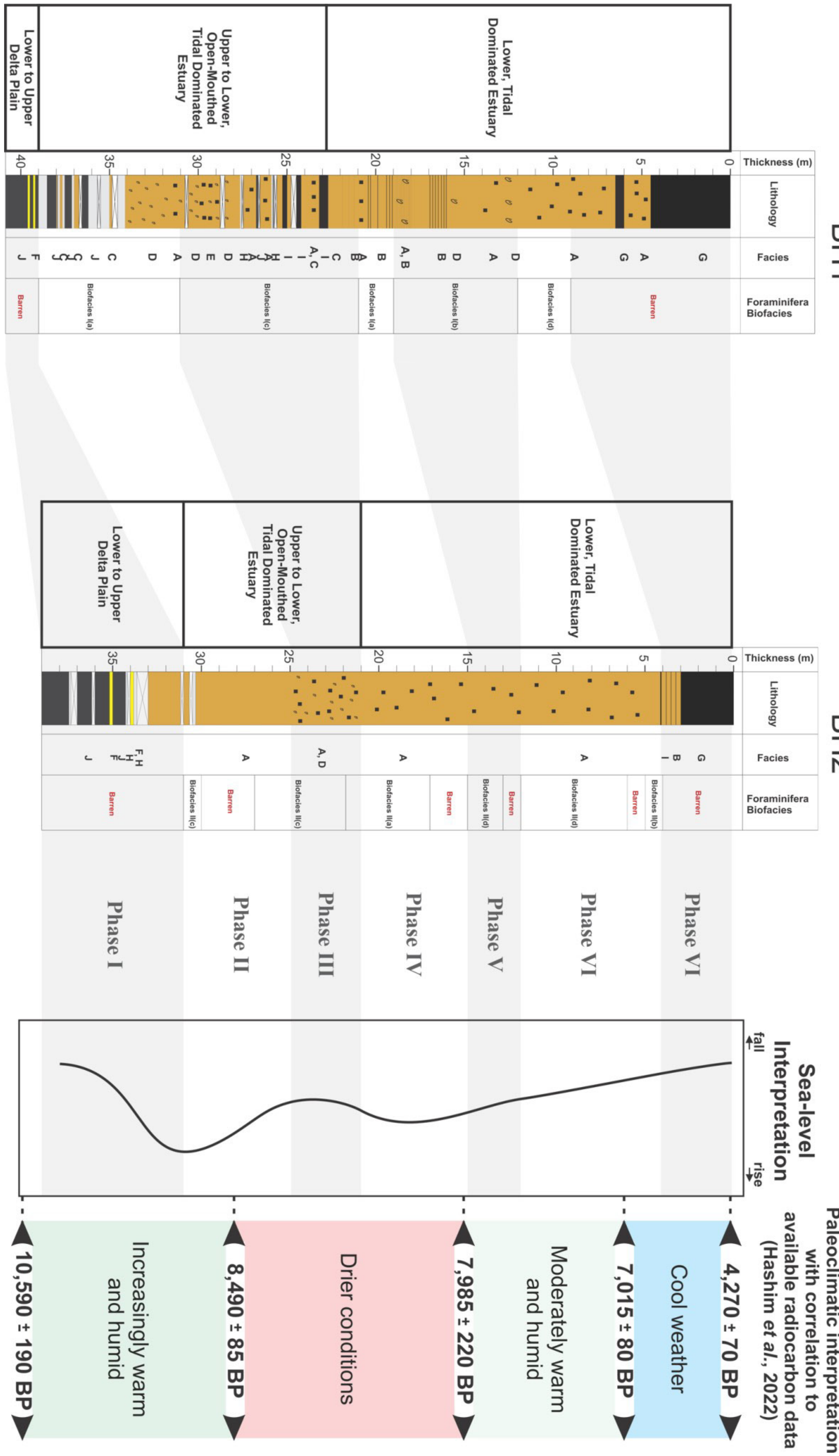

Figure 11: Interpretation of sea-level changes in western Johor with correlated radiocarbon age constraint from Hashim *et al.* (2022).

REFERENCES

Abdullah, S., Kamaludin, B.H., & Tjia, H.D., 2003. The Holocene optimum in Malaysia. Minerals and Geoscience Department Malaysia Technical Papers, 2, 37–67.

Abouelresh, M., & Slatt, R. 2011. Shale depositional processes: Example from the Paleozoic Barnett Shale, Fort Worth Basin, Texas, USA. Open Geosciences, 3(4), 398-409.

Ali, T.A., 2010. Analysis of shoreline-changes based on the geometric representation of the shorelines in the GIS database. Journal of Geography and Geospatial Information Science, 1(1), 1-16.

Amorosi, A.,Bruno, L., Cleveland, D., Morelli, A., & Hong, W., 2016. Paleosols and associated channel-belt sand bodies from a continuously subsiding late Quaternary system (Po Basin, Italy): New insights into continental sequence stratigraphy. Geological Society of America Bulletin, 129, B31575.1.

Azmi, M.Y., & Kamaludin, H., 1997. Palynology of late Quaternary coastal sediments, Perak, Malaysia. Catena, 30, 391-406.

Barnett, E.J., & Harvey, N., 2001. Relative sea-level change and geologic corrections to South Australian tide gauge records. In: Noye, B.J., & Grzechnik, M.P. (Eds.), Sea-level changes and their effects. Ocean and Atmosphere Pacific: OAP95. World Scientific Publishing Co., Singapore, 95–124.

Bird, M.I., Taylor, D., & Hunt, C., 2005. Palaeoenvironments of insular Southeast Asia during the Last Glacial Period: A savanna corridor in Sundaland? Quaternary Science Reviews, 24, 2228–2242.

Bird, M.I., Fifield, L.K., Teh, T.S., Chang, C.H., Shirlaw, N., & Lambeck, K., 2007. An inflection in the rate of early mid-Holocene eustatic sea-level rise: A new sea-level curve from Singapore. Estuarine, Coastal and Shelf Science, 71, 523–536.

Bird, M.I., Austin, W.E.N., Wurster, C.M., Fifield, L.K., Mojtahid, M., & Sargeant, C., 2010. Punctuated eustatic sea-level rise in the early mid-Holocene. Geology, 38, 803–806.

Biswas, B., 1973. Quaternary changes in sea-level in the South China Sea. Bulletin of the Geological Society of Malaysia, 6, 229 – 256.

Blum, M., Martin, J., Milliken, K., & Garvin, M., 2013. Paleovalley systems: Insights from Quaternary analogs and experiments. Earth-Science Reviews, 116, 128–169.

Bosch, J.H.A., 1988. The Quaternary deposits in the coastal plains of Peninsular Malaysia. Geological Survey Malaysia Quaternary Geology Report 1/86.

Bosch, J.H.A., 1989. Quaternary geologic map of Peninsular Malaysia. Geological Survey of Malaysia Publication.

Catuneanu, O., Abreu, V., Bhattacharya, J.P., Blum, M.D., Dalrymple, R.W., Eriksson, P.G., Fielding, C.R., Fisher, W.L., Galloway, W.E., Gibling, M.R., Giles, K.A., Holbrook, J.M., Jordan, R., Kendall, C.G.St.C., Macurda, B., Martinsen, O.J., Miall, A.D., Neal, J.E., Nummedal, D., Pomar, L., Posamentier, H.W., Pratt, B.R., Sarg, J.F., Shanley, K.W., Steel, R.J., Strasser, A., Tucker, M.E., & Winker, C., 2009. Towards the standardization of sequence stratigraphy. Earth-Science Reviews, 92 (1–2), 1-33.

Che Aziz, A., 2002. Sedimentary sequence in the subsurface of the Pekan coastal plain, Pahang. Proceedings of the Geological Society of Malaysia Annual Geological Conference 2002.

Chen, S., Steel, R.J., & Olariu, C., 2015. Paleo-Orinoco (Pliocene) channels on the tide-dominated Morne L'Enfer delta lobes and estuaries, SW Trinidad. In: Ash-worth, P.J., Best, J.L., & Parsons, D.R. (Eds.), Fluvial-tidal sedimentology. Developments in Sedimentology, 68, 227–281.

Clayton, J.A., & Pitlick, J., 2008. Persistence of the surface texture of a gravel-bed river during a large flood. Earth Surface Processes and Landforms, 33(5), 661-673.

Crucifix, M., Braconnot, P., Harrison, S.P., & Otto-Bliesner B., 2005. Second phase of paleoclimate modelling intercomparison project, Eos Trans. AGU, 86, 264.

Culver, S., Mallinson, D., Corbett, D., Leorri, E., Rouf, A., Shazili, N.A.M., Yaacob, R., Whittaker, J., Buzas, M., & Parham, P., 2012. Distribution of foraminifera in the Setiu estuary and lagoon, Terengganu, Malaysia. The Journal of Foraminiferal Research, 42, 109-133.

Daidu, F., Wang, Y., & Liu, M., 2013. Classifications, sedimentary features and facies associations of tidal flats. Journal of Palaeogeography, 2(1), 66-80.

Dalrymple, R.W., 2022. A review of the morphology, physical processes and deposits of modern straits. Geological Society London Special Publications, 523(1), SP523-2021.

Dalrymple, R.W., Knight R.J., Zaitlin B.A., & Middleton G.V., 1990. Dynamics and facies model of a macrotidal sand bar complex. Sedimentology, 35, 577–612.

Dalrymple, R.W., Baker, E.K., Harris, P.T., & Hughes, M.G., 2003. Sedimentology and stratigraphy of a tide-dominated, foreland-basin delta (Fly River, Papua New Guinea). In: Sidi, F.H., Nummedal, D., Imbert, P., Darman, H., & Posamentier, H.W. (Eds.), Tropical deltas of Southeast Asia-Sedimentology, Stratigraphy, and Petroleum Geology. Society for Sedimentary Geology (SEPM) Special Publication, 76, 147–173.

Dalrymple, R.W., 2006. Incised valleys in space and time: An introduction to the volume and an examination of the controls on valley formation and filling. In: Dalrymple, R.W., Leckie, D.A., & Tillman R.W. (Eds.), Incised valleys in space and time. SEPM Society for Sedimentary Geology Special Publication, 85, 5–12.

Dalrymple, R.W., Mackay, D.A., Ichaso, A.A., & Choi, K.S., 2012. Processes, morphodynamics, and facies of tide-dominated estuaries. In: Davis, R.A., Jr., & Dalrymple, R.W. (Eds.), Principles of tidal sedimentology. Springer, New York. 621 p.

Davis, J.H.,1940. The ecology and geologic role of mangroves in Florida. Carnegie Institution of Washington Pub., 32, 305–412.

Davis, R.A. Jr., & FitzGerald, D.M., 2009. Beaches and coasts. John Wiley & Sons, Malden, MA. 432 p.

Demicco, R.V., & Gierlowski-Kordesch, E.H., 1986. Facies sequences of a semi-arid closed basin; the Lower Jurassic East Berlin Formation of the Hartford Basin, New England, U.S.A. Sedimentology, 33, 107–118.

Diessel, C.F.K., 1992. Coal-bearing depositional systems. Springer, Berlin, Germany. 721 p.

Dietrich, W.E., & Smith, J.D., 1984. Bed load transport in a river meander. Water Resources Research, 20(10), 1355– 1380.

Dowsett, H., Dolan, A., Rowley, D., Moucha, R., Forte, A.M., Mitrovica, J.X., Pound, M., Salzmann, U., Robinson, M., Chandler, M., Foley, K., & Haywood, A., 2016. The PRISM4 (mid-Piacenzian) paleoenvironmental reconstruction. Climate of the Past, 12, 1519–1538.

Freytet, P., & Verrecchia, E.P., 2002. Lacustrine and palustrine carbonate petrography: An overview. Journal of Paleolimnology, 27(2), 221-237.

Fujimoto, K., Miyagi, T., Kikuchi, T., & Kawana. T., 1996. Mangrove habitat formation and response to Holocene sea-level changes on Kosrae Island. Micronesia Mangrove Salt Marshes, 1, 47–57.

Fujimoto, K., Miyagi, T., Murofushi, T., Mochida, Y., Umitsu, M., Adachi, H., & Pramojanee, P., 1999a. Mangrove habitat dynamics and Holocene Sea-level changes in the southwestern coast of Thailand. Tropics, 8, 239–255.

Fujimoto, K., Miura, M., Kobayashi, S., & Simbolon, H., 2019. Habitat evolution of a peat swamp forest and belowground carbon sequestration during the Holocene along the coastal lowland in Central Sumatra, Indonesia. Progress in Earth and Planetary Science, 6(1), 1-13.

Freytet, P., & Verrecchia, E.P., 2002. Lacustrine and palustrine carbonate petrography: An overview. Journal of Paleolimnology, 27(2), 221-237.

Gallop, S.L., Kennedy, D.M., Loureiro, C., Naylor, L.A., Muñoz-Pérez, J.J., Jackson, D.W., & Fellowes, T.E., 2020. Geologically controlled sandy beaches: Their geomorphology, morphodynamics and classification. Science of the Total Environment, 139123.

Genchi, S.A., Vitale, A.J., Perillo, G.M.E., Seitz, C., & Delrieux, C.A., 2020. Mapping topobathymetry in a shallow tidal environment using low-cost technology. Remote Sens., 12, 1394.

Geng, L., Gong, Z., Zhou, Z., Lanzoni, S., & D'Alpaos, A., 2020. Assessing the relative contributions of the flood tide and the ebb tide to tidal channel network dynamics. Earth Surface Processes and Landforms, 45(1), 237-250.

Geyh, M.A., Kudrass, H.R., & Streif, H., 1979. Sea-level changes during the late Pleistocene and Holocene in the Strait of Malacca. Nature, 278, 441–443.

Goddéris, Y., Donnadieu, Y., Le, Hir. G., & Lefebvre, V., 2014. The role of palaeogeography in the Phanerozoic history of atmospheric CO_2 and climate. Earth-Science Reviews, 128, 122–138.

Goñi, M.A., Teixeira, M.J., & Perkey, D.W., 2003. Sources and distribution of organic matter in a river-dominated estuary (Winyah Bay, SC, USA). Estuarine, Coastal and Shelf Science, 57(5-6), 1023-1048.

Golonka, J., Ross, M.I., & Scotese, C.R., 1994. Phanerozoic paleogeographic and paleoclimatic modeling maps. In: Embry, A.F., Beauchamp, B., & Glass, D.J. (Eds.), Pangea: Global environment and resources. Memoir-Canadian Society of Petroleum Geologists, 17, 1–47.

Gray, L.M., Basir J., & Tjia, H.D., 1978. Fossils at Sri Medan, Johor. Warta Geologi, 4, 81-84.

Gustavson, T.C., 1991. Arid basin depositional systems and paleosols: Fort Hancock and Camp Rice Formations (Pliocene-Pleistocene), Hueco Bolson, West Texas and Adjacent Mexico. The University of Texas at Austin, Bureau of Economic Geology, Report of Investigations No. 198, 49 p.

Hall, R., van Hattum, M.W.A., & Spakman, W., 2008. Impact of India–Asia collision on SE Asia: The record in Borneo. Tectonophysics, 451, 366–389.

Hall, R., 2014. The origin of Sundaland. Proceedings of Sundaland Resources 2014. MGEI Annual Convention, 17-18 November 2014, Palembang, South Sumatra, Indonesia.

Hammer, O., Harper, D.A.T., & Ryan, P.D., 2001. PAST: paleontological statistics software package for education and data analysis. Palaeontologia Electronica, 4(1), 1–9.

Hanebuth, T., Stattegger, K., & Grootes, P.M., 2000. Rapid flooding of the Sunda Shelf: A late-glacial sea-level record. Science, 288, 1033–1035.

Hanebuth, T.J.J., Stattegger, K., & Saito, Y., 2002. The stratigraphic architecture of the central Sunda Shelf (SE Asia) recorded by shallow-seismic surveying. Geo-Marine Letters, 22, 86-94.

Hanebuth, T.J.J., & Stattegger, K., 2004. Depositional sequences on a late Pleistocene–Holocene tropical siliciclastic shelf (Sunda Shelf, southeast Asia). Journal of Asian Earth Sciences, 23, 113-126.

Hanebuth, T.J.J., Voris, H.K., Yokoyama, Y., Saito, Y., & Okuno, J., 2011. Formation and fate of sedimentary depocentres on Southeast Asia's Sunda Shelf over the past sea-level cycle and biogeographic implications. Earth Science Reviews, 104, 92-110.

Hashim, A.H., Jamil, H., & Omar, R., 2022. Clay minerals and their implications for Late Quaternary palaeoclimate investigation: A case study in Pontian, Johor. Bulletin of the Geological Society of Malaysia, 73, 91-103.

Hasmadi, I.M., Pakhriazad, H.Z., & Norlida, K., 2011. Remote sensing for mapping RAMSAR heritage site at Sungai Pulai Mangrove Forest Reserve, Johor, Malaysia. Sains Malaysiana, 40(2), 83-88.

Heaney, L.R., 1991. A synopsis of climatic and vegetational change in southeast Asia. Climatic Change, 19, 53–61.

Hesp, P.A., Hung, C.C., Hilton, M., Ming, C.L., & Turner, I.M., 1998. A first tentative Holocene sea-level curve for Singapore. Journal of Coastal Research, 14, 308–314.

Holbrook, J.M., & Bhattacharya, J.P., 2012. Reappraisal of the sequence boundary in time and space: Case and considerations for an SU (subaerial unconformity) that is not a sediment bypass surface, a time barrier, or an unconformity. Earth-Science Reviews, 113, 271–302.

Horton, B.P., Benjamin, P., Gibbard, L.G., Milne, M., Morley, R.J., Purintavaragul, C., & Stargardt, J.M., 2005. Holocene sea levels and palaeoenvironments, Malay-Thai Peninsula, Southeast Asia. The Holocene, 15, 1199-1213.

Ichaso, A.A., & Dalrymple, R.W., 2009. Tide- and wave-generated fluid mud deposits in the Tilje Formation (Jurassic), offshore Norway. Geology, 37, 539–542.

Jain, S., Abdelhady, A.A., & Alhussein, M., 2019. Responses of benthic foraminifera to environmental variability: A case from the Middle Jurassic of the Kachchh Basin (Western India). Marine Micropaleontology, 151, 101749.

Jiang, C., Wu, Z., Chen, J., Deng, B., & Long, Y., 2015. Sorting and sedimentology character of sandy beach under wave action. Procedia Engineering, 116, 771-777.

Kamaludin, H., 1993. The changing mangrove shoreline in Kuala Kurau, Peninsular Malaysia. In: C.D. Woodroffe (Ed.), Late Quaternary evolution of coastal and lowland riverine plains of Southeast Asia and Northern Australia. Sedimentary Geology, 83, 187–197.

Kamaludin, B.H., 2002. Holocene sea level changes in Peninsular Malaysia. Bulletin of the Geological Society of Malaysia, 45, 301-307.

Kamaludin, B. H., 2003. Mid-Holocene to recent sea level changes in Peninsular Malaysia: A tectonic implication. Bulletin of the Geological Society of Malaysia, 46, 313-318.

Khan, N.S., Ashe, E., Horton, B.P., Dutton, A., Kopp, R.E., Brocard, G., Engelhart, S.E., Hill, D.F., Peltier, W.R., Vane, C.H., & Scatena, F.N., 2017. Drivers of Holocene sea-level change in the Caribbean. Quaternary Science Reviews, 155, 13-36.

Khan, N.S., Horton, B.P., Engelhart, S., Rovere, A., Vacchi, M., Ashe, E.L., Törnqvist, T.E., Dutton, A., Hijma, M.P., & Shennan, I., 2019. Inception of a global atlas of sea levels since the Last Glacial Maximum. Quaternary Science Reviews, 220, 359-371.

Khoo, T., 1996. Geomorphological evolution of the Merbok estuary area and its impact on the early state of Kedah, northwest Peninsular Malaysia. Journal of Southeast Asian Earth Sciences, 13(3-5), 347-371.

Kirby, R., & Parker, W.R., 1983. Distribution and behavior of fine sediment in the Severn Estuary and inner Bristol Channel, U.K. Canadian Journal of Fisheries and Aquatic Sciences, 40, 83–95.

Kudrass, H.R., & Schluter, H.U., 1994. Development of cassiterite bearing sediments and their relation to late Pleistocene sea level changes in the Straits of Malacca. Marine Geology, 120, 175-202.

Kvale, E.P., 2012. Tidal constituents of modern and ancient tidal rhythmites: Criteria for recognition and analyses. In: Davis, R.A. Jr., & Dalrymple, R.W. (Eds.), Principles of tidal sedimentology. Springer, Dordrecht. 621 p.

Law, W.M., 1970. Generalized soil map Peninsular Malaysia. Soil Survey Division, Ministry of Agriculture and Fisheries, Malaysia.

Leuven, J.R.F.W., Kleinhans, M.G., Weisscher, S.A.H., & van der Vegt, M., 2016. Tidal sand bar dimensions and shapes in estuaries. Earth-Science Reviews, 161, 204–233.

Lindbo, D.L., Stolt, M.H., & Vepraskas, M.J., 2010. Redoximorphic features. In: G. Stoops, V. Marcelino, & F. Mees (Eds.), Interpretation of micromorphological features of soils and regoliths. Elsevier, Amsterdam, the Netherlands. 1000 p.

Lindholm, R.C., 1987. Grain size. In: Lindholm, R.C. (Ed.), A practical approach to sedimentology. Springer, Dordrecht. https://doi.org/10.1007/978-94-011-7683-5.

Lindholm, R.C., 2012. A practical approach to sedimentology. Springer Science & Business Media, Vancouver. 291 p.

Liu, Z., Colin, C., Huang, W., Le, K.P., Tong, S., Chen, Z., & Trentesaux, A., 2007. Climatic and tectonic controls on weathering in South China and the Indochina Peninsula: Clay mineralogical and geochemical investigations from the Pearl, Red, and Mekong drainage basins. Geochemistry, Geophysics, Geosystems, 8(5). https://doi.org/10.1029/2006GC001490.

Loucks, R.G., & Ruppel, S.C., 2007. Mississippian Barnett Shale: Lithofacies and depositional setting of a deep-water shale-gas succession in the Fort Worth Basin, Texas. AAPG Bulletin, 91(4), 579-601.

MacKay, D.A., & Dalrymple, R.W., 2011. Dynamic mud deposition in a tidal environment: The record of fluid-mud deposition in the Cretaceous Bluesky Formation, Alberta, Canada. Journal of Sedimentary Research, 81(12), 901–920.

Mallinson, D., Culver, S., Corbett, D., Parham, P., Shazili, M., Azhar, N., & Rosnan, Y., 2014. Holocene coastal response to monsoons and relative sea-level changes in northeast Peninsular Malaysia. Journal of Asian Earth Sciences, 91, 194-205.

Martin, J., Cantelli, A., Paola, C., Blum, M., & Wolinsky, M., 2011. Quantitative modeling of the evolution and geometry of incised valleys. Journal of Sedimentary Research, 81, 64–79.

McCabe, P., 2009. Depositional environments of coal and coal-bearing strata. In: R.A. Rahmani, & R.M. Flores (Eds.), Sedimentology of coal and coal-bearing sequences. John Wiley & Sons. 368 p.

McCabe, A.M., Dardis, G.F., & Hanvey, P.M., 1984. Sedimentology of a late Pleistocene submarine-moraine complex, County Down, Northern Ireland. Journal of Sedimentary Research, 54(3), 716-730.

Miall, A.D., 1996. The geology of fluvial deposits: Sedimentrary facies, basin analysis, and petroleum geology. Springer, Berlin, Heidelberg, New York, London, Paris, Tokyo, Hong Kong. 582 p.

Minhat, F.I., Satyanarayana, B., Husain, M.L., & Rajan, V.V.V., 2016. Modern benthic foraminifera in subtidal waters of Johor: Implications for Holocene sea-level change on the East Coast of Peninsular Malaysia. Journal of Foraminiferal Research, 46(4), 347–357.

Mohd Hasmadi, I., Pakhriazad, H.Z., & Norlida, K., 2011. Remote sensing for mapping RAMSAR heritage site at Sungai Pulai Mangrove Forest Reserve, Johore, Malaysia. Sains Malaysiana, 40(2), 83–88.

Mulamba, T., Bacopoulos, P., Kubatko, E., & Pinto, G., 2019. Sea-level rise impacts on longitudinal salinity for a low-gradient estuarine system. Climatic Change, 152(3-4), 533-550.

Murray, J.W., 2003. An illustrated guide to the benthic foraminifera of the Hebridean shelf, west of Scotland, with notes on their mode of life. Palaeontologia Electronica, 5(1), 31.

Nanson, G.C., 1980. Point bar and floodplain formation of the meandering Beatton River, northeastern British Columbia, Canada. Sedimentology, 27, 3-29.

Noorbergen, L.J., Abels, H.A., Hilgen, F.J., Robson, B.E., de Jong, E., Dekkers, M.J., Krijgsman, W., Smit, J., Collinson, M.E., & Kuiper, K.F., 2018. Conceptual models for short-eccentricity-scale climate control on peat formation in a lower Palaeocene fluvial system, north-eastern Montana (USA). Sedimentology, 65(3), 775-808.

Parham, P.R., 2016. Late Cenozoic relative sea-level highstand record from Peninsular Malaysia and Malaysian Borneo: Implications for vertical crustal movements. Bulletin of the Geological Society of Malaysia, 62, 91-115.

Parham, P.R., Saito, Y., Noraisyah, S., Rokiah, S., & Noor Azariyah, M., 2014. Evidence for ca. 7 ka maximum Holocene transgression on the Peninsular Malaysia east coast. Journal of Quaternary Science, 29, 414-422.

Parham, P.R., Noraisyah, S., Rokiah, S., & Noor Azariyah, M., 2014b. Holocene relative sea-level highstand patterns, Peninsular Malaysia east coast. Abstracts with Programs, Geological Society of America Annual Meeting. Vancouver, BC, Canada.

Peterson, J.M., & Bell, S.S., 2012. Tidal events and salt-marsh structure influence black mangrove (Avicennia germinans) recruitment across an ecotone. Ecology, 93, 1648–1658.

Peterson, J.M., & Bell, S.S., 2015. Saltmarsh boundary modulates dispersal of mangrove propagules: Implications for mangrove migration with sea-level rise. PLoS ONE, 10(3), e0119128.

Plummer, P.S., & Gostin, V.A., 1981. Shrinkage cracks: Desiccation or syneresis? J. Sed. Petrol., 51, 1147–1156.

Retallack, G., 2001. Soils of the past, an introduction to pedology. Blackwell, Oxford. 600 p.

Saintilan, N., Khan, N.S., Ashe, E., Kelleway, J.J., Rogers, K., Woodroffe, C.D., & Horton, B.P., 2020. Thresholds of mangrove survival under rapid sea level rise. Science, 368(6495), 1118-1121.

Salles, T., Flament, N., & Müller, D., 2017. Influence of mantle flow on the drainage of eastern Australia since the Jurassic Period. Geochem. Geochemistry, Geophysics, Geosystems, 18(1), 280-305.

Sathiamurthy, E., & Voris, H.K., 2006. Maps of Holocene sea level transgression and submerged lakes on the Sunda Shelf. The Natural History Journal of Chulalongkorn University, Supplement, 2, 1-43.

Scholl, D.W., & Stuiver, M., 1967. Recent submergence of southern Florida: A comparison with adjacent coasts and other eustatic data. Geological Society of America Bulletin, 78, 437–454.

Shan, X., Shi, X., Qiao, S., Jin, L., Otharán, G.A., Zavala, C., Liu, J., Zhang, Y., Zhang, D., Xu, T., & Fu, C., 2019. The fluid mud flow deposits represent mud caps of Holocene hybrid event beds from the widest and gentlest shelf. Marine Geology, 415, 105959.

Shennan, I., Bradley, S., & Edwards, R., 2018. Relative sea-level changes and crustal movements in Britain and Ireland since the Last Glacial Maximum. Quaternary Science Reviews, 188, 143-159.

Short, A.D., 1991. Macro-meso tidal beach morphodynamics - An overview. Journal of Coastal Research, 7(2), 417–436.

Sinsakul, S., Sonsuk, M., & Hasting, P.J., 1985. Holocene sea levels in Thailand: Evidence and basis for interpretation. Journal of the Geological Society of Thailand, 8, 1–12.

Sinsakul, S., 1992. Evidence of Quaternary sea level changes in the coastal areas of Thailand: A review. Journal of Southeast Asian Earth Sciences, 7, 23–37.

Smoot, J.P., 1983. Depositional subenvironments in an arid closed basin; Wilkins Peak Member of the Green River Formation (Eocene), Wyoming, U.S.A. Sedimentology, 30, 801–827.

Supardi, Subekty, A.D., & Neuzil, S.G., 1993. General geology and peat resources of the Siak Kanan and Bengkalis Island peat deposits, Sumatra, Indonesia. In: Cobb, J.C., & Cecil, C.B. (Eds.), Modern and ancient coal-forming environments. Geological Society of America Special Paper, 286, 45–61.

Tam, C.Y., Zong, Y., Hassan, K., bin Ismal, H., Jamil, H., Xiong, H., Wu, P., Sun, Y., Huang, G., & Zheng, Z., 2018. A below-the-present late Holocene relative sea level and the glacial isostatic adjustment during the Holocene in the Malay Peninsula. Quaternary Science Reviews, 201, 206–222.

Taylor, D., Saksena, P., Sanderson, P.G., & Kucera, K., 1999. Environmental change and rain forests on the Sunda shelf of Southeast Asia: Drought, fire and the biological cooling of biodiversity hotspots. Biodiversity & Conservation, 8(9), 1159-1177.

Tessier, B., 1993. Upper intertidal rhythmites in the Mont-Saint-Michel Bay (NW France): Perspectives for paleoreconstruction. Marine Geology, 110(3-4), 355- 367.

Tjia, H.D., 1992. Holocene sea-level changes in the Malay-Thai Peninsula, a tectonically stable environment. Bulletin of the Geological Society of Malaysia, 31, 157-176.

Tjia, H.D., 1996. Sea-level changes in the tectonically stable Malay-Thai Peninsula. Quaternary International, 31, 95-101.

Tjia, H.D., 2001. The rate of geological processes: Natural modifications and destruction of the environment. Universiti Kebangsaan Malaysia, Lestari lecture 30.

Tjia, H.D., 2004. Accelerated shoreline growth and landscape development in Sungai Muda coastal plain. Warisan Geologi, 6, 195-206.

Tjia, H.D., & Sharifah Mastura, S.A., 2013. Sea level changes in Peninsular Malaysia: A geological perspective. Penerbit Universiti Kebangsaan Malaysia, Bangi. 150 p.

Tucker, M.E., 2003. Sedimentary rock in the field. John Wiley and Sons Ltd. 228 p.

Van den Berg, J.H., Boersma, J.R., & Gelder, A.V., 2007. Diagnostic sedimentary structures of the fluvial-tidal transition zone–Evidence from deposits of the Rhine and Meuse. Netherlands Journal of Geosciences, 86(3), 287-306.

Vital, H., Gomes, M.P., Tabosa, W.F., Frazão, E.P., Santos, C.L.A., & Placido, Junior_J.S., 2010. Characterization of the Brazilian continental shelf adjacent to Rio Grande Do Nortestate, Ne Brazil. Brazilian Journal of Oceanography, 58, 43–54.

Voris, H.K., 2000. Maps of Pleistocene sea levels in Southeast Asia: Shorelines, river systems and time durations. Journal of Biogeography, 27(5), 1153–1167.

Wang, R., Colombera, L., & Mountney, N.P., 2019. Geological controls on the geometry of incised-valley fills: Insights from a global dataset of late-Quaternary examples. Sedimentology, 66, 2134–2168.

Wilmes, S.B., Schmittner, A., & Green, J.A.M., 2019. Glacial ice sheet extent effects on modeled tidal mixing and the global overturning circulation. Paleoceanography and Paleoclimatology, 34, 1437– 1454.

Woodroffe, S.A., & Horton, B.P., 2005. Holocene sea-level changes in the Indo-Pacific. Journal of Asian Earth Sciences, 25, 29-43.

Zhang, L., Buijsman, M.C., Comino, E., & Swinney, H.L., 2017. Internal wave generation by tidal flow over periodically and randomly distributed seamounts, Journal of Geophysical Research: Oceans, 122(6), 5063-5074.

Manuscript received 29 June 2021;
Received in revised form 26 October 2022;
Accepted 1 November 2022
Available online 30 November 2022